

# Berichte

zur Polar-  
und Meeresforschung

591  
2009

Reports  
on Polar and Marine Research



The Expedition of the Research Vessel "Polarstern"  
to the Antarctic in 2008 (ANT-XXIV/4)

---

Edited by  
Andreas Macke  
with contributions of the participants



HELMHOLTZ  
| GEMEINSCHAFT

ALFRED-WEGENER-INSTITUT FÜR  
POLAR- UND MEERESFORSCHUNG  
In der Helmholtz-Gemeinschaft  
D-27570 BREMERHAVEN  
Bundesrepublik Deutschland

ISSN 1866-3192

# Hinweis

Die Berichte zur Polar- und Meeresforschung werden vom Alfred-Wegener-Institut für Polar- und Meeresforschung in Bremerhaven\* in unregelmäßiger Abfolge herausgegeben.

Sie enthalten Beschreibungen und Ergebnisse der vom Institut (AWI) oder mit seiner Unterstützung durchgeführten Forschungsarbeiten in den Polargebieten und in den Meeren.

Es werden veröffentlicht:

- Expeditionsberichte (inkl. Stationslisten und Routenkarten)
- Expeditionsergebnisse (inkl. Dissertationen)
- wissenschaftliche Ergebnisse der Antarktis-Stationen und anderer Forschungs-Stationen des AWI
- Berichte wissenschaftlicher Tagungen

Die Beiträge geben nicht notwendigerweise die Auffassung des Instituts wieder.

# Notice

The Reports on Polar and Marine Research are issued by the Alfred Wegener Institute for Polar and Marine Research in Bremerhaven\*, Federal Republic of Germany. They appear in irregular intervals.

They contain descriptions and results of investigations in polar regions and in the seas either conducted by the Institute (AWI) or with its support.

The following items are published:

- expedition reports (incl. station lists and route maps)
- expedition results (incl. Ph.D. theses)
- scientific results of the Antarctic stations and of other AWI research stations
- reports on scientific meetings

The papers contained in the Reports do not necessarily reflect the opinion of the Institute.

The „Berichte zur Polar- und Meeresforschung“  
continue the former „Berichte zur Polarforschung“

## \* Anschrift / Address

Alfred-Wegener-Institut  
Für Polar- und Meeresforschung  
D-27570 Bremerhaven  
Germany  
[www.awi.de](http://www.awi.de)

Editor in charge:  
Dr. Horst Bornemann

Assistant editor:  
Birgit Chiaventone

Die "Berichte zur Polar- und Meeresforschung" (ISSN 1866-3192) werden ab 2008 ausschließlich elektronisch als Open-Access-Publikation herausgegeben (URL: <http://epic.awi.de>).

**The Expedition of the Research Vessel "Polarstern"  
to the Antarctic in 2008 (ANT-XXIV/4)**

---

**Edited by  
Andreas Macke  
with contributions of the participants**

**Ber. Polarforsch. Meeresforsch. 591 (2009)  
ISSN 1866-3192**



**ANT-XXIV/4**  
**18 April 2008 - 20 May 2008**  
**Punta Arenas - Bremerhaven**

**Fahrtleiter / Chief Scientist**  
**Andreas Macke**

---

**Koordinator / Coordinator**  
**Eberhard Fahrbach**



---

## **CONTENTS**

<b>1. Fahrverlauf und Zusammenfassung</b>	<b>7</b>
<b>Cruise narrative and summary</b>	<b>10</b>
<b>2. Weather conditions</b>	<b>12</b>
<b>3. NITRATLANTIK 08: Study of the isotope composition of marine and atmospheric nitrate in the Atlantic Ocean</b>	<b>18</b>
<b>4. Autonomous measurement platforms for energy and material exchange between ocean and atmosphere (OCEANET) - atmosphere component</b>	<b>25</b>
<b>5. Autonomous measurement platforms for energy and material exchange between ocean and atmosphere (OCEANET) - ocean component</b>	<b>33</b>
<b>6. Aerosols</b>	<b>39</b>
<b>7. ADCP measurements</b>	<b>43</b>
<b>8. Final sea trial and calibration of the Atlas Hydrosweep multibeam echosounder during ANT-XXIX/4, Las Palmas - Bremerhaven (12.05.2008 - 20.05.2008)</b>	<b>44</b>
<b>9. Sea trial and testing of the new upgraded deep sea sediment echo sounder “PARASOUND DS III-P70” during ANT-XXIV/4 (third phase)</b>	<b>46</b>

---

<b>10. Satellite ground truth: bio-optical and atmospheric studies</b>	<b>49</b>
<b>10.1 Bio-optical measurements</b>	<b>49</b>
<b>10.2. MAX-DOAS measurements of atmospheric trace gases and water reflectance</b>	<b>52</b>
<b>11. Long-term changes of abyssal temperatures in the Vema Channel</b>	<b>54</b>
<b>APPENDIX</b>	<b>58</b>
<b>A.1 Beteiligte Institute/ Participating institutions</b>	<b>59</b>
<b>A.2 Fahrtteilnehmer / Cruise participants</b>	<b>61</b>
<b>A.3 Schiffsbesatzung / Ship's crew</b>	<b>62</b>
<b>A.4 Stationsliste / Station list PS 71</b>	<b>63</b>

---

## **1. FAHRTVERLAUF UND ZUSAMMENFASSUNG**

A. Macke  
IFM-GEOMAR

Am 18. 4. 2008 pünktlich um 19:00 Uhr Ortszeit legte *Polarstern* vom Hafen Punta Arenas ab und fuhr auf direktem Kurs nach Bremerhaven mit Stop in Las Palmas, um Personal zur Kalibrierung und Durchführung von Testläufen des Hydrosweep D2-Systems an Bord zu nehmen. Im Vema-Kanal wurde eine vollständige CTD-Messung bis zum Meeresboden durchgeführt, die zur Langzeiterfassung der dekadischen Schwankungen des Antarktischen Bodenwassers beiträgt. Neben der 42köpfigen Besatzung waren 19 Wissenschaftler und 2 Mitarbeiter des DWD an Bord.

Ein Großteil der Arbeiten bestand in der kontinuierlichen Erfassung des Zustands der Atmosphäre, der biochemischen Eigenschaften des oberen Ozeans und der Energie- und Stoffflüsse zwischen beiden und wurde im Rahmen des WGL-Verbundprojektes OCEANET durchgeführt. Die Phyto-Optik-Gruppe des AWI und der Universität Bremen hat das spektrale Lichtangebot unter Wasser gemessen, ergänzt durch die Beobachtung der Unterwasserlichtfluktuation der Atmosphärengruppe des IFM-GEOMAR. Die Lichtdaten der Phyto-Optik-Gruppe wurden gemeinsam mit Tiefenprofilen der Phytoplanktonkonzentration untersucht, um einen möglichen Zusammenhang zwischen der Verteilung der verschiedenen Phytoplanktonarten und dem vorhandenen Lichtangebot herzustellen.

Ein MAXDOAS Spektralradiometer erfasste die bodennahen Spurengase. Mit Hilfe eines Luftsammlers mit angeschlossenem Filtersystem wurde das bodennahe Aerosol großenteils gesammelt und später isotopisch analysiert.

Schließlich fand ein betreuter Transport der in Chile beheimateten Krebsarten *Paralomis granulosa* und *Lithodes santolla* zwecks Untersuchungen am AWI statt.

Die Atmosphärengruppe war mit der Messung des atmosphärischen Aerosols, der Feuchte- und Temperaturprofile, der Bewölkung, der solaren und thermischen Einstrahlung sowie der turbulenten Flüsse von Impuls, Wärme, Wasserdampf und CO<sub>2</sub> beschäftigt.

Die Radiosondenaufstiege, die die DWD-Mitarbeiter jeden Tag um 12:00 UTC durchführten, boten eine sehr gute Gelegenheit zur Validierung des „Humidity and Temperature Profiler“ HATPRO Multikanalmikrowellenradiometers. Während der Überflüge des europäischen Wettersatelliten MetOp wurden im Auftrag von EUMETSAT zusätzliche Radiosondenaufstiege zur Validierung des Radiometers IASI durchgeführt.

Die Messungen der optischen Dicke des Aerosols sind Bestandteil des gerade gegründeten „Marine Aerosol Network“ der NASA. Die Atlantik-Profile der *Polarstern* liefern zur Zeit die größte Datenmenge für dieses Netzwerk.

Zur Erfassung der vertikalen turbulenten Flüsse von Impuls, Wasserdampf und CO<sub>2</sub> zwischen Ozean und Atmosphäre wurden drei zeitlich hochauflösende Geräte zur Messung der drei Windgeschwindigkeitskomponenten und der jeweiligen Gaskonzentrationen am Krähennest montiert.

Per Filtration wurden Proben zur Untersuchung mariner Stickstofffixierer gewonnen. Einen weiteren Forschungsschwerpunkt bildeten unizelluläre Stickstofffixierer.

Mit der Ferry Box des GKSS-Forschungszentrums wurden ozeanographische Parameter, wie Salzgehalt und Temperatur, aber auch Parameter, die Informationen über biologische Prozesse im Meer liefern, aufgezeichnet.

Die OCEAN-Gruppe des IFM-GEOMAR hat in einem Durchflussbecken den Gesamtgasdruck aller im Seewasser gelösten Gase und mittels einer Sauerstoffoptode den gelösten Sauerstoff gemessen. Aus diesen Parametern lässt sich unter anderem der Gasaustausch zwischen Ozean und Atmosphäre bestimmen.

ANT-XXIV/4 war eine sehr erfolgreiche Fahrt und verlief ohne nennenswerte Probleme. Das Wetter und die See haben insbesondere bei den Lichtmessungen hervorragend mitgespielt.

Im Namen der beteiligten Wissenschaftler danke ich Kapitän Schwarze und seiner Besatzung für die exzellente Unterstützung während der gesamten Fahrt.

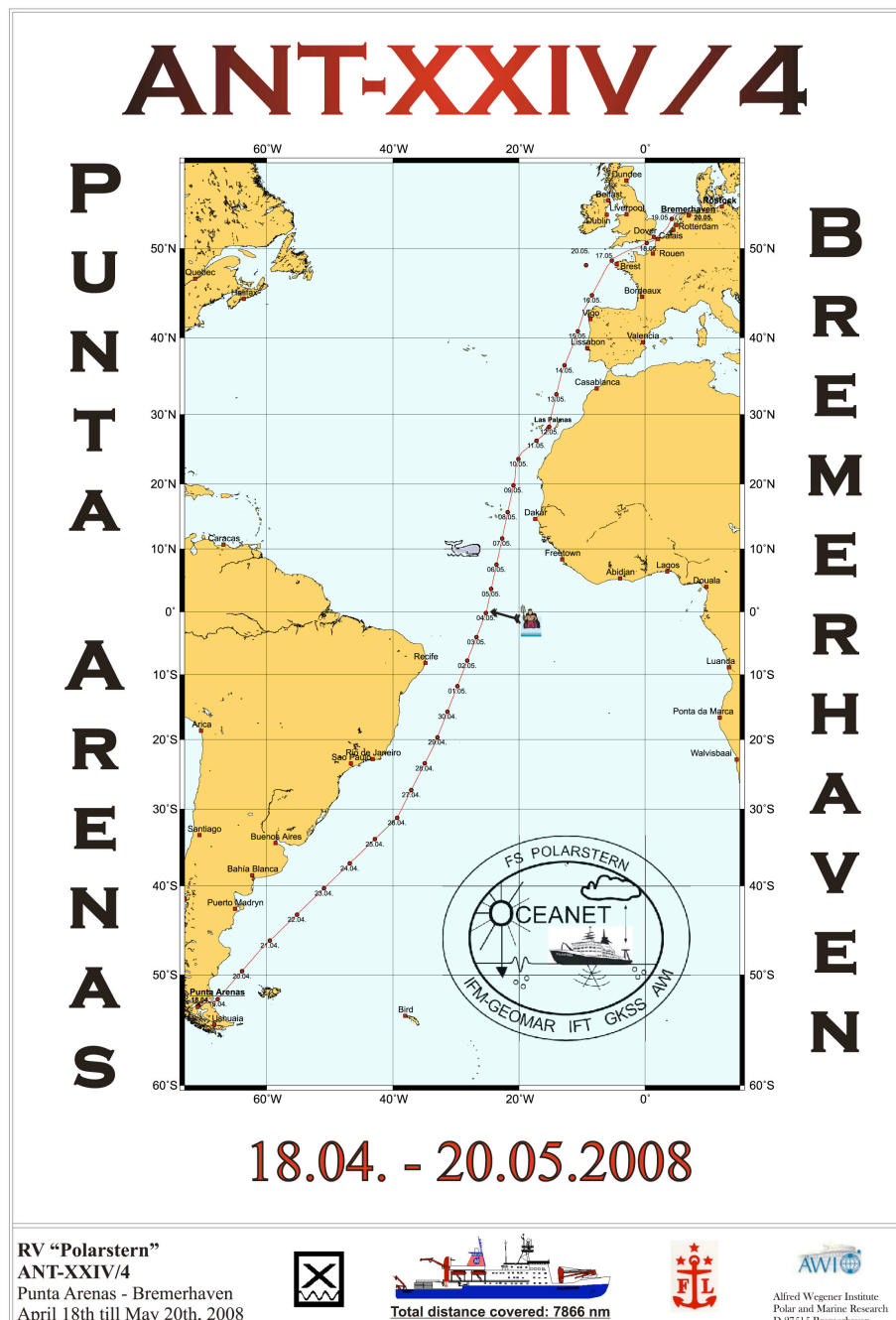


Abb. 1: Fahrtroute der Polarstern während der Expedition ANT-XXIV/4  
 Fig. 1: Cruise track of Polarstern section ANT-XXIV/4

---

## CRUISE NARRATIVE AND SUMMARY

On 18 April 2008 at 19:00 local time the research vessel *Polarstern* left the harbour of Punta Arenas heading directly to Bremerhaven with one stop in Las Palmas to board personnel for the calibration and sea trial of the Hydrosweep D2-system. A full CTD measurement to the ocean bottom was carried out at the Vema channel. The observation contributed to the long-term monitoring of decadal variations in the Antarctic Bottom Water. On board there were 42 crew members, 19 scientists and 2 two staff members of the DWD.

A major part of the work consisted in the continuous observation of the atmosphere, the biochemical properties of the upper ocean and the energy and material exchange between ocean and atmosphere. These measurements have been performed in the framework of the WGL joint project OCEANET.

The phyto-optics group at the AWI and the University of Bremen performed measurements of the submarine spectral light availability, supplemented by observations of submarine light fluctuations from the atmosphere group of IFM-GEOMAR. The radiation data from the phyto-optics group were analyzed together with profiles of phyto-plankton concentrations in order to obtain a relation between the distribution of different plankton species and the existing light availability.

Surface-near trace gases were retrieved with a MAXDOAS spectral radiometer. By means of an air volume sampler with attached filter system the surface near aerosol was collected in various size classes for later isotopic analysis.

Finally, an attended transportation of the Chilenean crab species *Paralomis granulosa* and *Lithodes santolla* was carried out for later analysis at AWI.

The atmosphere group was engaged in the measurements of atmospheric aerosol, the temperature and humidity profiles, the cloudiness, the solar and thermal irradiance as well as the turbulent fluxes of heat, humidity and CO<sub>2</sub>.

The radiosonde ascents carried out by the DWD crew each day at 12:00 UTC provided an excellent opportunity to validate the „Humidity and Temperature Profiler“ HATPRO microwave radiometer. During the overpasses of the European weather satellite MetOp additional radiosondes had been launched for validation of the radiometer IASI onboard MetOp.

The observations of the aerosol optical thickness are part of the recently established „Marine Aerosol Network“ of NASA. Up to now the Atlantic transects of *Polarstern* have provided the largest data set for this network.

In order to retrieve the turbulent fluxes of momentum, water vapour, and CO<sub>2</sub> three instruments with high temporal resolution were mounted on the crows net that measured wind speed and the corresponding gas concentrations.

By means of filtration samples of marine nitrate fixer were obtained. Another focus was laying in uni-cellular nitrate fixer.

Oceanographic parameters like salinity, temperature, and parameters that contain information on biological processes in the ocean had been recorded with the Ferry Box of the GKSS research center.

Total gas pressure of all gases dissolved in the sea water was measured in a through-flow basin by the IFM-GEOMAR Ocean group. By means of an oxygen optode the dissolved oxygen was retrieved. From these parameters the gas exchange between ocean and atmosphere can be determined.

ANT-XXIV/4 had been a very successful cruise without any noteworthy problems. Especially the weather and see conditions during the light observations had been very favourable.

On behalf of the participating scientists I like to thank Master Schwarze and his crew for the excellent support during the entire cruise.

## 2. WEATHER CONDITIONS

Eugen Müller  
DWD Deutscher Wetterdienst Hamburg

In the evening of 18 April *Polarstern* left Punta Arenas and began the cruise ANT-XXIV/4 back to Bremerhaven. Northwesterly winds 5 Bft were caused by an intermediate high that passed over to the east. But already on the next day an extensive storm cyclone developed west of the Antarctic Peninsula (Fig. 2.1) and a northerly wind increased up to 9 Bft and waves of 6 m were observed.

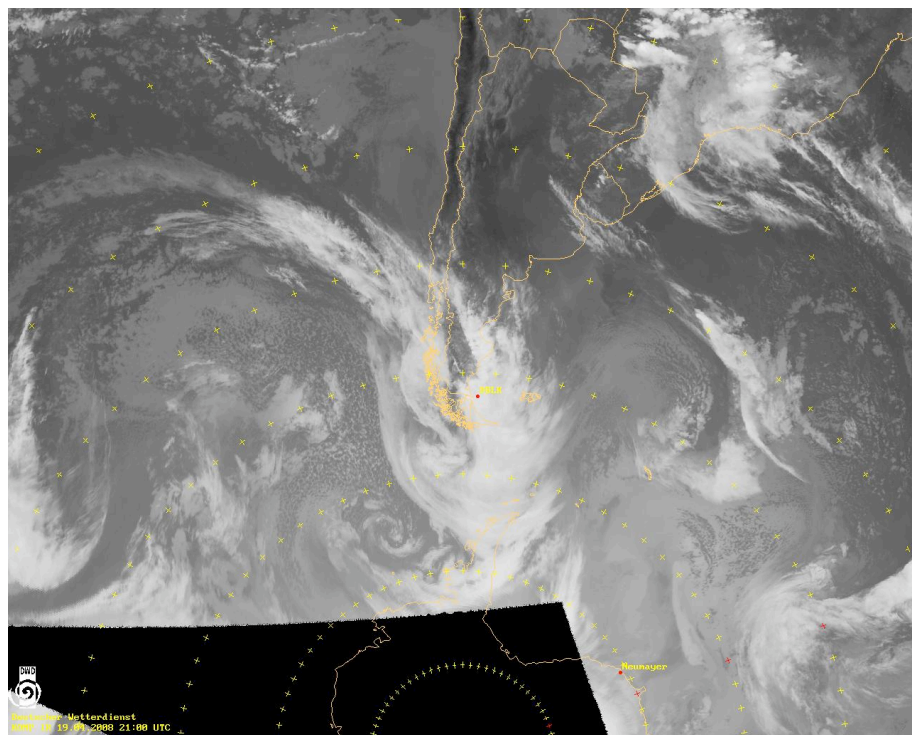
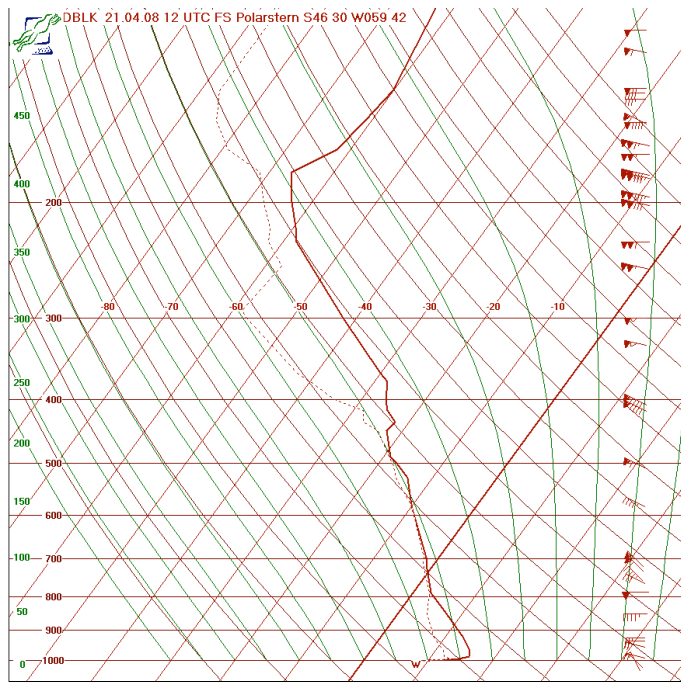


Fig. 2.1: The storm cyclone with its centre west of the Antarctic Peninsula  
(METEOSAT 19 April 2008 21 UTC)

On 20 April the cyclone moved further to the Weddell Sea and in a flat trough, that remained left, the wind decreased down to 3 Bft until the evening and shifted to southwest and later to south. On 21 April *Polarstern* was still in this flat trough (with an embedded frontal zone) originating from the low over the Weddell Sea. Because of the relatively cold water of the Falkland Current a very pronounced inversion in the lowest layer formed and later fog with a visibility partly less than 100 m (Fig. 2.2, 2.3).

*Fig. 2.2: Patches of cold water fog (21 April)*



*Fig. 2.3: Radiosounding of Polarstern 21 April 2008 12 UTC*

On 22 and 23 April a flat zone of high pressure over the South Atlantic north of 40°S dominated and brought south- to southwesterly winds of 4 Bft.

On 24 April a secondary cyclone near the Falkland Islands deepened to a storm low. It became then the steering centre of the extensive low pressure system over the Weddell Sea. As a consequence the huge low pressure system expanded further to the north and reached also *Polarstern* with its circulation. Westerly winds of 5 Bft increased to 7 Bft (waves 4 m) on 25 April. On the following day the low went back to the south (centre near South Sandwich Islands) and the wind decreased to 4 Bft.

With further proceeding to the north *Polarstern* came more and more under the influence of the subtropical high pressure system with its centre west of South Africa. But until 29 April the vertical stratification was still unstable, because of a long wave trough in the upper levels extending from the polar region to 20°S. Deep convection with showers of rain and thunderstorms developed. The trade winds became prevailing with a wind speed of 4 - 5 Bft.

From 30 April to 3 May *Polarstern* crossed the trade winds current. The typically southeasterly to easterly winds dominated with wind speeds of 4 Bft, temporary 5 Bft. The swell decreased slowly from 2,5 m to 1,5 m. The air and water temperature were around 28 °C.

At this time the innertropical convergence zone (ITCZ) was embedded in the equatorial trough ran along the equator, partly more to the north to 3°N. On 4 and 5 May *Polarstern* crossed the equatorial trough (Fig. 2.4). Although the typically moist und unstable airmass (Fig. 2.5) in this region would have favoured deep convection, there were only a few showers of rain and some sheet lightning far away when *Polarstern* passed the ITCZ. The main convective activity with its thunderstorms in the ITCZ was concentrated in the Gulf of Guinea.

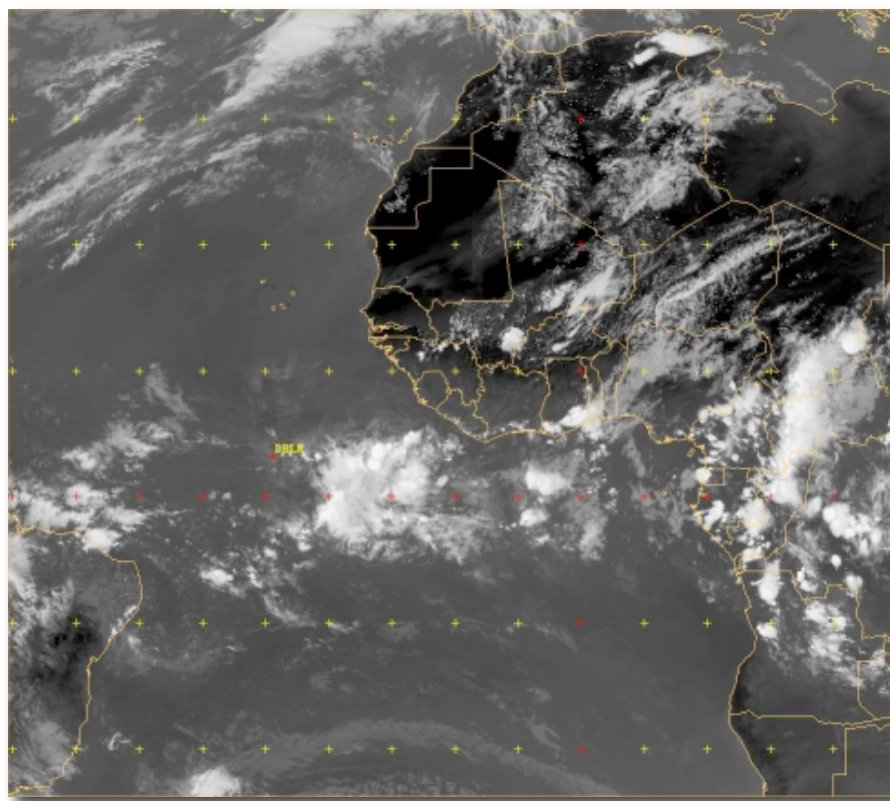


Fig. 2.4: The position of the ITCZ on 5 May 2008 15 UTC (METEOSAT)

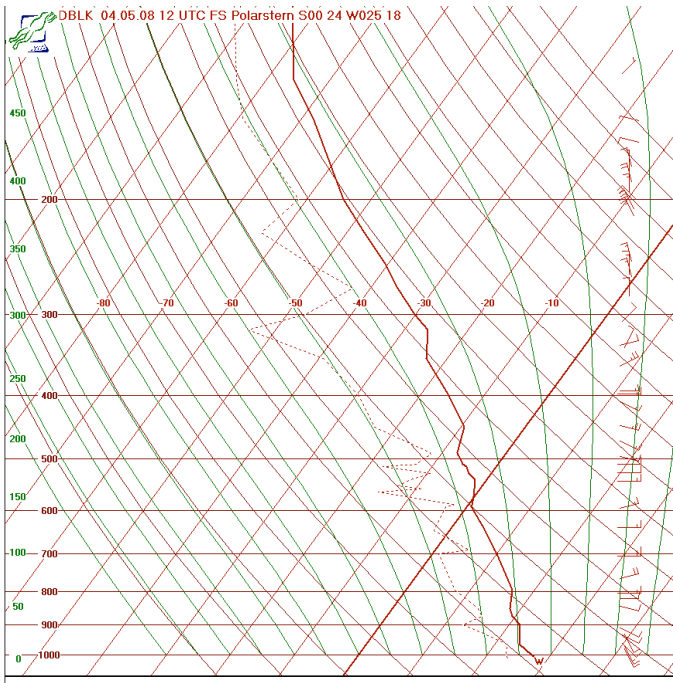
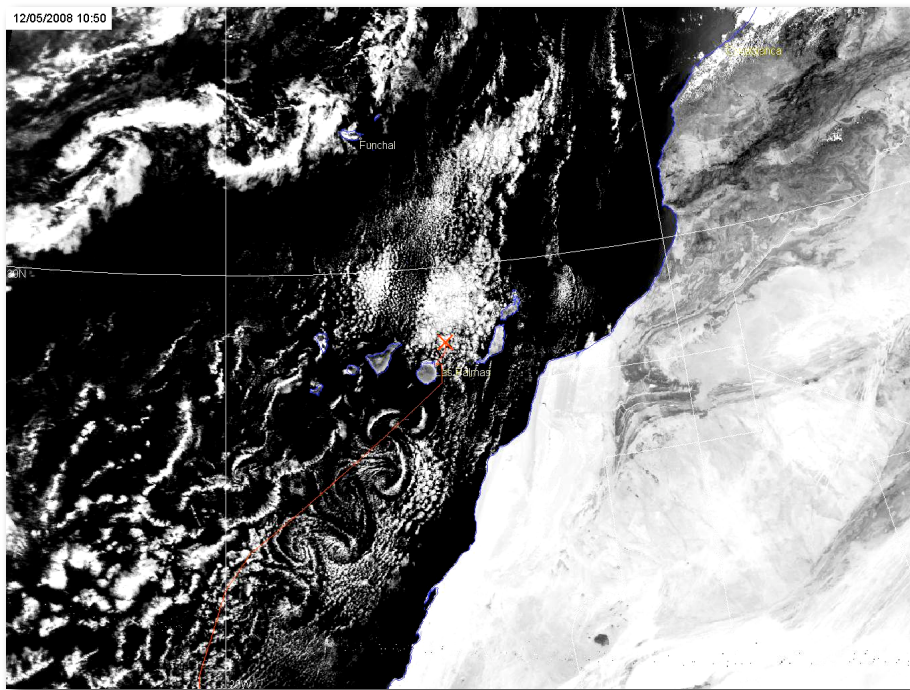


Fig. 2.5: Radiosounding of  
4 May 2008 12 UTC

From 7 to 11 May the northeasterly trade winds were prevailing. They were maintained by the subtropical anticyclone with its centre southwest of the Azores, shifting slowly towards Madeira, and by a persisting heat low over the Sahara. The wind speed was around 5 Bft, temporary up to 6 Bft (9/10 May) and the wave height was around 2.5 m. The air and water temperature decreased continually to 20 °C.

On 11 May the well-known phenomena of the Karman vortex streets downstream of the Canary Islands could be observed very well (Fig. 2.6). *Polarstern* crossed the vortex streets northeastwards, what resulted in big variations of wind speed. The wind changed regularly every 1,5 - 2 hours from NE-N with 3 - 4 Bft to E with 5 - 6 Bft (Fig. 2.7). Corresponding variations of the pressure, the temperature and the relative humidity could be also observed.



*Fig 2.6: Karman vortex streets downstream of the Canary Islands  
(NOAA15 11 May 2008 18:25 UTC)*

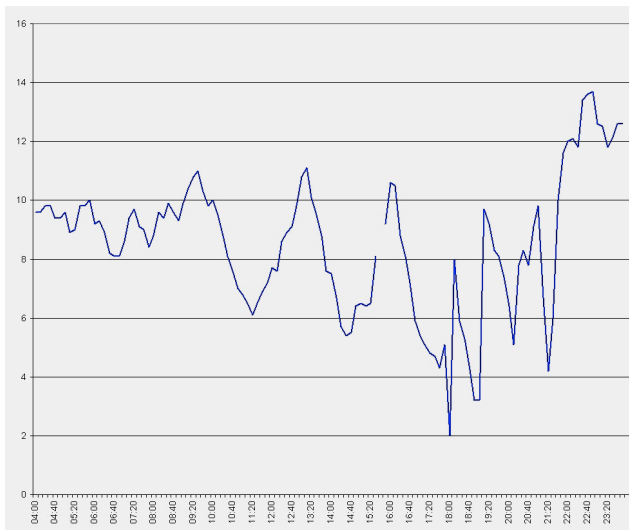


*Fig. 2.7: Time series of wind speed  
(m/s) when Polarstern crossed the  
Karman vortex streets*

In the morning of 12 May *Polarstern* called at the port of Las Palmas for the embarkation of some technicians of the Alfred Wegener Institute. On this day moderate northerly winds of 4 Bft prevailed. On the following days a subtropical anticyclone south of the Azores remained stationary. A small low, a former secondary cyclone, moved driven by an upper-low towards the Biscay. Its weak coldfront passed *Polarstern* on the afternoon of 13 May and brought a shower of rain. On 14 and 15 May the low pressure system in the Biscay moved very slowly eastwards.

Because of the small pressure gradients there were only moderate W-NW winds of 4 Bft, but a swell of 2 - 2,5 m could be observed.

The pressure field during the cruise through the Biscay and the English Channel (16 -18 May) was defined by a flat low, that extended from Spain to the Baltic. An embedded weak vortex moved, steered by an upper low, from the Biscay to Germany and further to the Baltic. On 18 May the cold front of a cyclone over the Baltic Sea crossed the English Channel southwards. In the cold polar air behind this front a ridge of high pressure built up over the British Isles. On 16 and 17 May west-northwesterly winds prevailed with wind speeds of 3 - 4 Bft. With the cold front passage on 18 May a northeasterly wind of 6 - 7 Bft sprang up (wave height 2,5 - 3 m).

On 19 May the ridge of high pressure shifted a little to the east over the North Sea. As a consequence northerly winds of 5 Bft accompanied *Polarstern* on the way through the North Sea. In the early morning of 20 May *Polarstern* reached Bremerhaven.

---

### **3. NITRATLANTIK 08: Study of the isotope composition of marine and atmospheric nitrate in the Atlantic Ocean**

Joseph Erbland

Laboratoire de Glaciologie et Géophysique de l'Environnement,

CNRS - UJF Grenoble, Grenoble, France (LGGE)

not on board: Samuel Morin and Joël Savarino

#### **Objectives**

The analysis of the isotopic composition of nitrate ( $\text{NO}_3^-$ ) in various environments (marine, atmospheric, ice cores ...) is a fast-growing field of investigation. Isotope measurements complement concentration data, which alone do not allow for a thorough understanding of the intricate cycling of nitrogen oxides at the surface of the Earth, and in particular in the atmosphere. The discovery that ozone, one of the most prominent oxidant in the atmosphere, could transfer its isotopic anomaly ( $\Delta^{17}\text{O} = ^{17}\text{O} - 0.52 \times \delta^{18}\text{O}$ , where  $\delta = R_{\text{sample}}/R_{\text{reference}} - 1$  and  $R$  is the  $^{17}\text{O}/^{16}\text{O}$ ,  $^{18}\text{O}/^{16}\text{O}$  or  $^{15}\text{N}/^{14}\text{N}$  ratio in the sample and in a reference material) to nitrogen oxides ( $\text{NO}_x$ , the precursors of nitrate), has brought to light the potential for atmospheric nitrate isotopes to be a proxy for the oxidative capacity of the atmosphere. Nitrogen isotope ratios are generally considered to behave as tracers of the  $\text{NO}_x$  sources.

Since the development of techniques able to accurately measure  $\Delta^{17}\text{O}(\text{NO}_3^-)$  is very recent, few measurements are available for atmospheric nitrate. In addition, polar regions have been targeted first because of the potential for reconstructing past levels of ozone (thus, past oxidative capacity of the atmosphere) through the measurement of  $\Delta^{17}\text{O}(\text{NO}_3^-)$  in ice and firn.  $\Delta^{17}\text{O}(\text{NO}_3^-)$  was also measured in polar atmospheres and has given indications about atmospheric processes such as boundary layer ozone depletion events. Only one pioneering study was aimed at unravelling the seasonal cycle of  $\Delta^{17}\text{O}$  in atmospheric nitrate in a mid-latitude, polluted marine boundary layer. The authors found that changes in  $\Delta^{17}\text{O}$  values were best accounted for by changes in oxidation pathways over the course of the year: for instance, in winter, enhanced formation of nitrate through nighttime heterogeneous processes such as the hydrolysis of  $\text{N}_2\text{O}_5$  leads to an increase in  $\Delta^{17}\text{O}$  values. In summer, the gas-phase reaction between the hydroxyl radical OH and  $\text{NO}_2$  leads to lower  $\Delta^{17}\text{O}$  values. Coupled studies of all three isotope ratios of nitrate, i.e.  $\delta^{15}\text{N}$ ,  $\delta^{17}\text{O}$  and  $\delta^{18}\text{O}$ , have shown that considerable insight is given by the dual interpretation of  $\delta^{15}\text{N}$  and  $\Delta^{17}\text{O}$  in atmospheric nitrate, in terms of sources and atmospheric processes, for atmospheric nitrate collected in the coastal Antarctica (Dumont d'Urville) over the course of a full year.

The ANT-XXIV/4 *Polarstern* cruise between Punta Arenas (Chile) and Bremerhaven (Germany) followed the ANT-XXIII/10 cruise between Cape Town (Rep. South Africa) and Bremerhaven (Germany). Thus, this cruise allowed for the second time to measure  $\delta^{15}\text{N}$ ,  $\delta^{17}\text{O}$  and  $\delta^{18}\text{O}$  in atmospheric nitrate collected in a wide range of meteorological and photochemical conditions, in the marine boundary layer of the Atlantic Ocean. This new data set will:

- enhance the global representation of the isotopic composition of atmospheric nitrate, both for oxygen and nitrogen in a wider range of latitudes and atmospheric conditions,
- place new constraints on the processes responsible for the formation of atmospheric nitrate in the marine boundary layer, in relation with latitudinal variations in atmospheric concentration oxidants such as ozone and OH (due, for instance, to changes in air-masses origin, actinic flux, temperature, humidity),
- provide some new information about nocturnal/diurnal influences in dusty and polluted conditions.

*Fig. 3.1: High-volume aerosol sampler during the ANT-XXIV/4 cruise onboard Polarstern*



## Work at sea

### Aerosol collection

Atmospheric particles (aerosol) were collected on the observation deck by means of high volume sampling (HiVol, see Fig. 3.1): a turbo-pump sucks in air through a filtering medium at a flow-rate of about  $1 \text{ m}^3 \text{ min}^{-1}$ . The air flows through an assemblage of four slotted plates (four-stage impactor), each of them bearing a slotted pre-cleaned glass fiber filter, on which particles are selectively deposited depending on their aerodynamic diameter. This allows to separate larger particles (diameter  $> 1 \mu\text{m}$ ), directly injected into the atmosphere such as sea spray, from smaller particles which can originate from a variety of pathways, including gas-to-particle conversions. Owing to generally calm and steady weather conditions, the sampling was carried out on a daily regular basis, hence the latitudinal resolution of these measurements is on the order of  $4^\circ$ .

Strong winds and heavy sea at the entrance of the Atlantic Ocean caused the delay of the aerosols collection. Therefore, the collection started on the 20 April, 2 days after the departure. Over the course of the ANT-XXIV/4 cruise, 21 series of filters were obtained, representing 42 samples to be analyzed in our laboratory in Grenoble:

indeed, the two slotted filters corresponding to the largest supermicron particles, SF1–2 (see figures 3.2(a) and 3.2(b)) are stored and analyzed together as are the bulk filters corresponding to the submicron mode (figure 3.2(e)). Two slotted filters corresponding to the smallest supermicron particles (SF3–4, Fig. 3.2(c) and 3.2(d)) were used to ensure the correct behaviour of the impactor but left for 7 days. Those filters will not be analyzed at our lab.

More, intensive collections were run twice to investigate for nocturnal/diurnal influences in the formation of nitrate. Filters were collected 4 times a day (every 6 hours) along the Sahara during 3 days to investigate for the influence of Saharan dust on nitrate formation. These 2 more intensive campaigns represented altogether 48 filters to be analyzed at our lab (24 of each filter: SF1–2, SF3–4 and the submicron filter). During the cruise, 6 sets of blanks were performed to assess the contamination induced by the handling of filters during their cleaning, shipping, storage and analysis. Blanks were treated identically to the samples, i.e., the filter-holder was loaded with regular filters, except that the HiVol was not turned on.

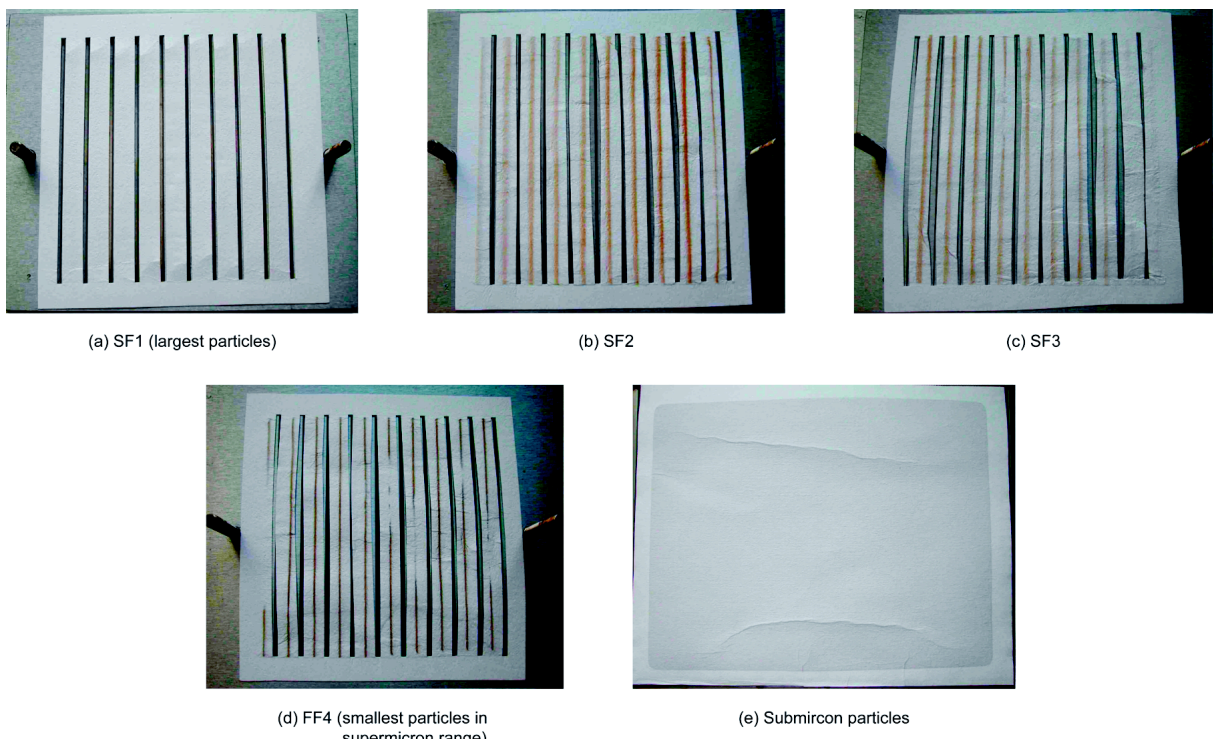


*Fig 3.2: Example of slotted (SF1–4) and backup (e) filters after 24 hours of sampling of aerosol containing dust from the Sahara*

### Surface ozone monitoring

Ozone was measured at a 10s resolution on the observation deck using a small UV-absorption ozone monitor (model 2020, 2B Technologies, Boulder CO, USA). Problems with the AC/DC converter were experienced during the first week of the cruise, resulting in a few days without measurements. The problem was fixed thanks to an extra converter borrowed onboard of the ship. Zero levels were checked

4 times during the cruise using a zero-ozone cartridge, and showed no variation in the offset value. A calibration will be performed to ensure the validity of the data acquired during the cruise.

### Results of the ANT XXIII/10 cruise

Since the samples collected during the ANT-XXIV/4 *Polarstern* cruise have not been analyzed yet, we briefly present here the meteorological, chemical and isotopic profiles measured from the collection performed during the ANT-XXIII/10 cruise (Fig. 3.4(a)). A wide range of types of air-masses and atmospheric conditions were observed during that cruise. Meteorological, backtrajectories (not shown) and chemical data allow for the discrimination of four areas featuring homogeneous air-masses properties (see Fig. 3.3). The South Atlantic Ocean (region 4) was first found to be a remote area with little biomass-burning and human influences. After the crossing of the ITCZ, region 3 was then influenced by dust emissions from the Sahara desert. Rain caused the removal of most of the nitrate in the atmosphere in region 2. Eventually, the last region (1) in the polluted English Channel had strong anthropogenic influences.

Ozone concentrations in the atmosphere show values from 2 to 2.5 times higher after the crossing of the ITCZ ( $4^{\circ}\text{N}$  at this period) than before it. Nitrate concentrations show an increase of total nitrate in the atmosphere with the latitude. The drop in region 2 is explained by precipitations that caused the removal of nitrate in the atmosphere. This rain also explains the occurrence of the low nitrate concentrations at the end of region 3 (before region 2). The mass distribution of nitrate (Fig. 3.4(b)) between submicron ( $<0.95\mu\text{m}$ ) and supermicron ( $>0.95\mu\text{m}$ ) modes shows that this last mode is predominant by 90% on average and even higher in low latitudes.

$\Delta^{17}\text{O}$  and  $\delta^{18}\text{O}$  values of nitrate (Fig. 3.4(b)) show an increase with latitude including a jump of some % after the crossing of the ITCZ. This suggests a change in the abundance and reactivity of the atmospheric particles on which heterogeneous reactions can happen. The comparison of  $\Delta^{17}\text{O}$  and  $\delta^{18}\text{O}$  nitrate values found in the Atlantic Oceans with the values found in polar regions (generally higher) shows that nitrate in the Atlantic is formed by the succession of nocturnal and diurnal processes

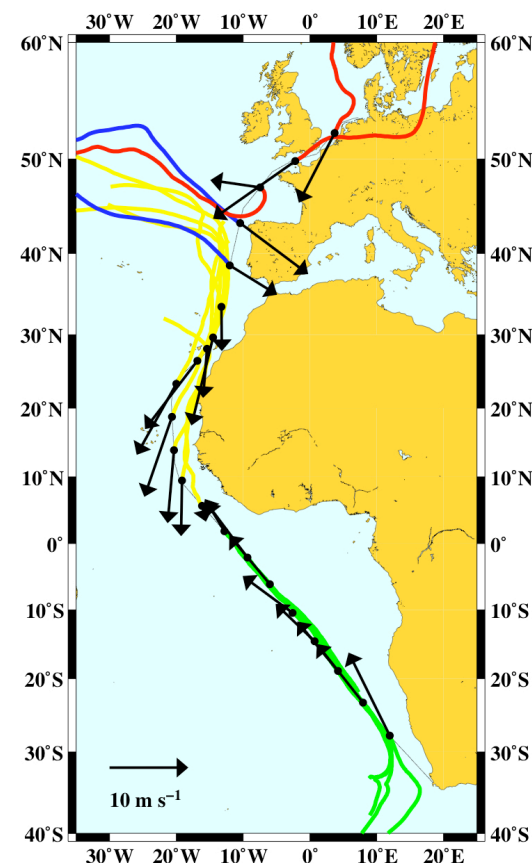


Fig. 3.3: ANT-XXII/10 *Polarstern* cruise track. The 4 regions are shown as well as the backtrajectories and the wind speeds and directions.

in the marine boundary layer. The discrimination between the supermicron and the submicron modes shows that heterogeneous mechanisms ( $\text{N}_2\text{O}_5$  hydrolysis) predominate in supermicron mode while homogeneous reactions (formation of nitrous acid by the reaction  $\text{OH}+\text{NO}_2$ ) are the most important in the submicron mode (see Fig. 3.4). Since nitrate is predominant in supermicron mode, heterogeneous mechanisms in nitrate formation have then the highest contribution.

$\delta^{15}\text{N}$  nitrate values eventually show a stable profile (-3‰) except in polluted areas where higher values (2 to 6‰) were measured. This shows 2 different sources of NOx in the atmosphere: natural sources (lightnings and biogenic sources) and humans activities. Submicron and supermicron modes do not show significant differences in tropical regions and northern mid-latitudes which suggest that the NOx sources are the same for these 3 modes.

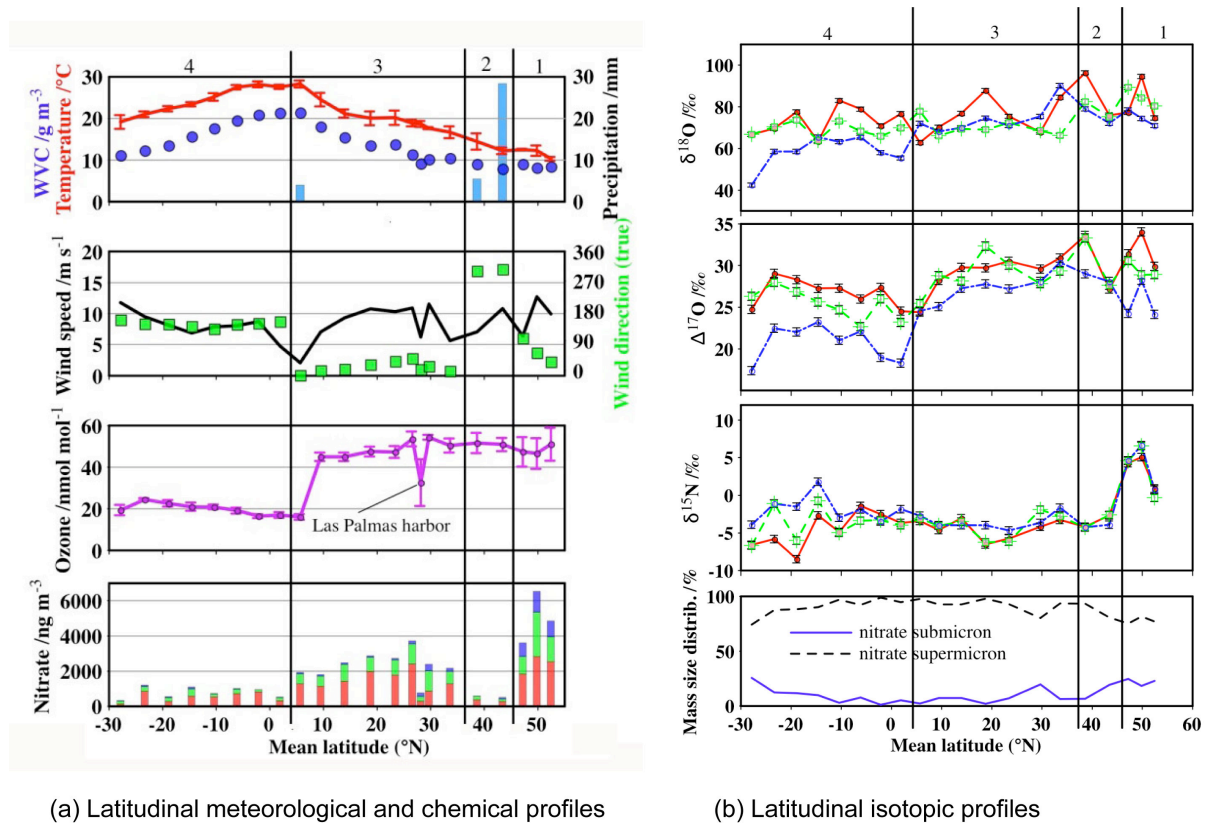


Fig. 3.4: Latitudinal profiles measured from the ANT-XXIII/10 Polarstern cruise collections (chemical profiles like concentrations of major ions, including  $\text{Cl}^-$ ,  $\text{SO}_4^{2-}$ ,  $\text{Ca}^{2+}$ ,  $\text{Na}^+$ ,  $\text{Mg}^{2+}$ ,  $\text{K}^+$ ,  $\text{NH}_4^+$  are missing). Red ( $>3\mu\text{m}$ ) and green ( $0.95\text{-}3\mu\text{m}$ ) colours represent supermicron mode while the blue colour represents submicron ( $<0.95\mu\text{m}$ ) mode.

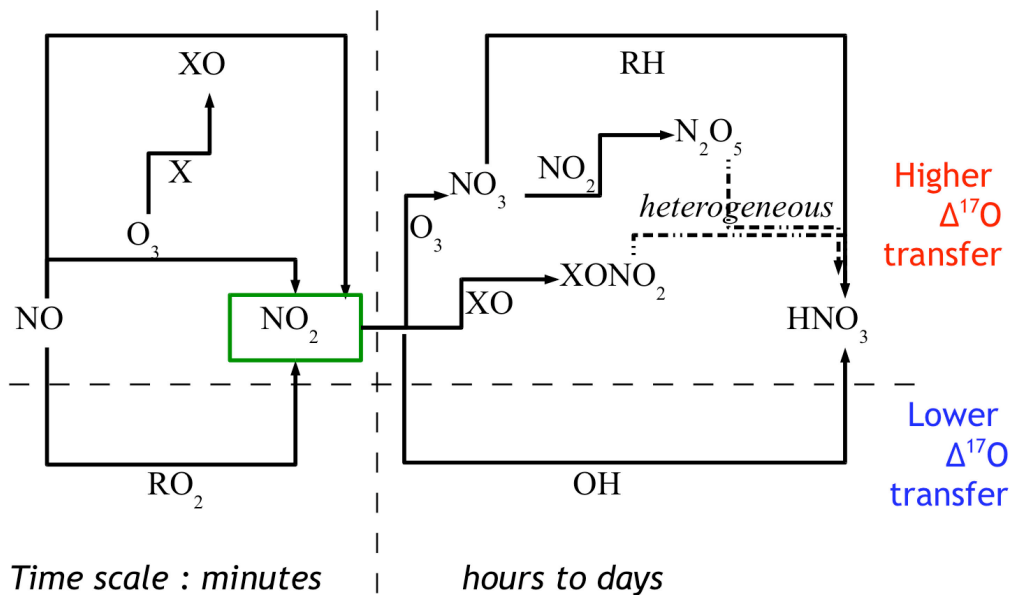


Fig. 3.5: Nitrate formation pathways and their influences on  $\Delta^{17}\text{O}$

## **Expected results of the ANT-XXIV/4 cruise**

It is expected this campaign to yield an additional comprehensive data set of  $\delta^{15}\text{N}$ ,  $\delta^{17}\text{O}$  and  $\delta^{18}\text{O}$  in atmospheric nitrate in the marine boundary layer of a wider range of latitudes (from 50°S to 53°N). To complement these observations, measurements of the concentration of major ions within the aerosol samples will be carried out (including  $\text{Cl}^-$ ,  $\text{NO}_3^-$ ,  $\text{SO}_4^{2-}$ ,  $\text{Ca}^{2+}$ ,  $\text{Na}^+$ ,  $\text{Mg}^{2+}$ ,  $\text{K}^+$ ,  $\text{NH}_4^+$ ).

A wide range of types of air-masses and atmospheric conditions were observed during this cruise. Shortly after the ship went out of the Magellan straight, a strong storm occurred with maximum wind speeds up to  $25 \text{ m.s}^{-1}$ . Heavy sea-sprays were blown on the observation deck so that it was impossible to set up the collecting system. Changing weather conditions occurred until 23 May when air masses were closely following the ship track for more than a day, as evidenced by real-time back-trajectories calculations provided by the German weather service (Deutscher Wetterdienst, DWD) on a daily basis. Then for 2 days, particles deposited on the slotted filters were almost impossible to see while particles deposited on the back-up filters were visible (possibly due to dust and pollutants emissions from South America). Ozone levels during this part of the cruise were rather low (on the order of  $27 \text{ nmol mol}^{-1}$ ). Such low values are compatible with the remote character of the air masses sampled during that time. However, the direction of the wind may have brought the ozone intake in contact with the exhaust plume of the ship's engine. Further studies will be aimed at determining whether NO emissions from the ship are sufficient to significantly destroy ambient ozone, hence, leading to an underestimation of surface ozone levels. It should be noted, however, that ship's exhaust is not likely to have contaminated the nitrate samples since the time scales for the conversion of NO<sub>x</sub> to nitrate are on the order of 1 day typically, much longer

than transport time scale from the ship's exhaust to the HiVol device (separated by 30 m approximately).

From 24 to 27 May, the wind blew from west leading to stable ozone levels but showers on the 26th. Back-trajectories from DWD showed air masses blown over South America. On the 28th, wind changed and blew from north. This direction slightly changed to east on the 30 and remained stable until 4 May. While this time, the ozone levels dropped to reach values as low as  $15 \text{ nmol mol}^{-1}$ .

On April 4 the equator was crossed and on the following day wind shifted to the north on a very abrupt manner; more waves were then encountered resulting in larger amounts of sea spray being injected into the atmosphere. On 6 May, filters exhibited brownish tints attributed to dust originating from North African deserts (e.g. Sahara, see Fig. 3.2). Ozone levels were then in the  $40 - 50 \text{ nmol mol}^{-1}$  range. The input of dust stopped the day after, but ozone levels remained in the same range.

From 13 May on, westerlies took over the trade wind (north-easterlies): in the area from Morocco to the entrance of the English Channel, the air masses were predominantly originating from the Northern Atlantic Ocean. There, ozone levels were on the order of  $50 \text{ nmol mol}^{-1}$  and the filters did not exhibit significant coloration.

The last intensive collection started on 16 May at 11:00 UTC around Cape Finisterre until 19 May at 11:00 UTC, before the arrival at Bremerhaven. On 17 May, the ship entered the British Channel: there, winds were mostly from the north-east. Ozone levels were still high (levels around  $50 \text{ nmol mol}^{-1}$  range) but dropped down to  $20 \text{ nmol mol}^{-1}$  for a few hours in the afternoon of 18 May. This event seems to correspond to air masses coming from the Arctic according to the back-trajectories provided by DWD. Aerosol filters in the British Channels showed soot particles in the smallest supermicron size range (SF4) and on the back-up filter.

---

## **4. AUTONOMOUS MEASUREMENT PLATFORMS FOR ENERGY AND MATERIAL EXCHANGE BETWEEN OCEAN AND ATMOSPHERE (OCEANET) - ATMOSPHERE COMPONENT**

Andreas Macke<sup>1)</sup>, Karl Bumke<sup>1)</sup>, John Kalisch<sup>1)</sup>, Martin Hieronymi<sup>1)</sup>, Yann Zoll<sup>1)</sup>, Katharina Lengfeld<sup>1)</sup>, Bernhard Pospichal<sup>2)</sup>, Stefan Kinne<sup>3)</sup>

<sup>1)</sup> IFM-GEOMAR

<sup>2)</sup> IGMK

<sup>3)</sup> MPI-Met

### **Objectives**

Clouds remain one of the biggest obstacles in our understanding of the coupled ocean-atmosphere climate system. Even under realistic forcing from observed wind, humidity and pressure fields climate models have difficulties to reproduce the correct spatial and temporal climatology of cloud cover. Because of the strong inhomogeneity of cloud pattern on those scales that are relevant for the radiative transfer processes it is clear that subgrid-scale processes must be accounted for in radiative transfer parametrizations. Combined observations of cloud physical and radiative properties are a key to adjust or to validate such parametrizations.

The turbulent fluxes of heat, momentum, humidity and CO<sub>2</sub> are measured to close the energy and mass budget at the sea surface. Most measurements are part of the Leibniz network-project OCEANET. A related goal is to quantify the role of clouds and sea surface wave on the small scale temporal and spatial variability of the solar radiation below the sea surface.

A further objective is to provide validation data for temperature and humidity profiles from the new infra-red sounding radiometer IASI on-board the first European polar orbiting operational weather satellite MetOp.

### **Work at sea**

The upward looking pyranometer Kipp&Zonen CM 21 and the pyrgeometer CG 4 operated by IFM-GEOMAR have been used on this cruise.

Every 15 seconds full sky images were obtained from a weather proofed digital camera system manufactured at IFM-GEOMAR. This enables a detailed analysis of the role of cloud cover and cloud type on the radiation budget at the sea surface.

As for the *Polarstern* transects ANT-XXIII/10, ANT-XXIV/1 and ANT-XXIV/4 a multi-channel microwave radiometer (HATPRO, radiometer physics) was utilized for continuous observations of atmospheric temperature and humidity profiles as well as liquid water and precipitable water path.

Together with ceilometer measurements of cloud bottom height, sun photometer measurements of aerosol optical thickness the data from the microwave radiometer provide a unique set of information to interpret the amount of downwelling solar and thermal radiation at the sea surface.

In addition to the continuous profiling by means of the HATPRO microwave radiometer, additional radiosondes had been launched whenever *Polarstern* was in the field of view of the IASI instrument on board MetOp.

A new instrument (Licor) to measure turbulent fluctuations of water vapor and CO<sub>2</sub> had been successfully installed and tested for measurements under marine conditions. Although the principle performance was satisfactory it turned out that electronic noise in the data transmission often produced spurious results. An older back-up instrument (M100) for observations of turbulent fluctuations of water vapor had been functioning properly for the entire cruise.

In collaboration with the Phyto-Optics Group of AWI and the University of Bremen the fluctuation of the spectral solar radiation at various depths was obtained from the RAMSES spectroradiometer of the AWI group. In order to quantify the spatial and temporal characteristics of these light fluctuations the brightness distribution on a white diffuse reflecting plate was filmed at various depths and will be spectrally analyzed later on. From this the characteristic space and time scales of the mostly surface wave induced light fluctuations was obtained as a function of sea condition and depth. An underwater camera system had been developed at IFM-GEOMAR that observes the light fluctuations projected on a white board at various depths. At the same time the sea surface tilts are determined by means of a light float. In a future step these data will be fed into a Monte-Carlo radiative transfer code to reproduce the observed spatial and temporal light fluctuations in the model.

### **Preliminary results**

Fig. 4.1 shows the time series of water vapor path (and liquid water path (LWP) along the cruise. The *in-situ* observed water vapor path or integrated water vapor (IVW) from the radiosonde measurements is also shown, and provides a generally good agreement with the indirectly obtained microwave products. Largest water vapor paths of more than 50 gm<sup>-2</sup> are observed at the thermal equator, where the warm conditions and strong cloud induced upwind pump most humidity from the ocean into the troposphere. The cloud LWP is given by the occasional data points above a background noise, which needs to be corrected during later analysis. The corrections make use of the sky camera images which indicate clear sky situations above the ship during day time.

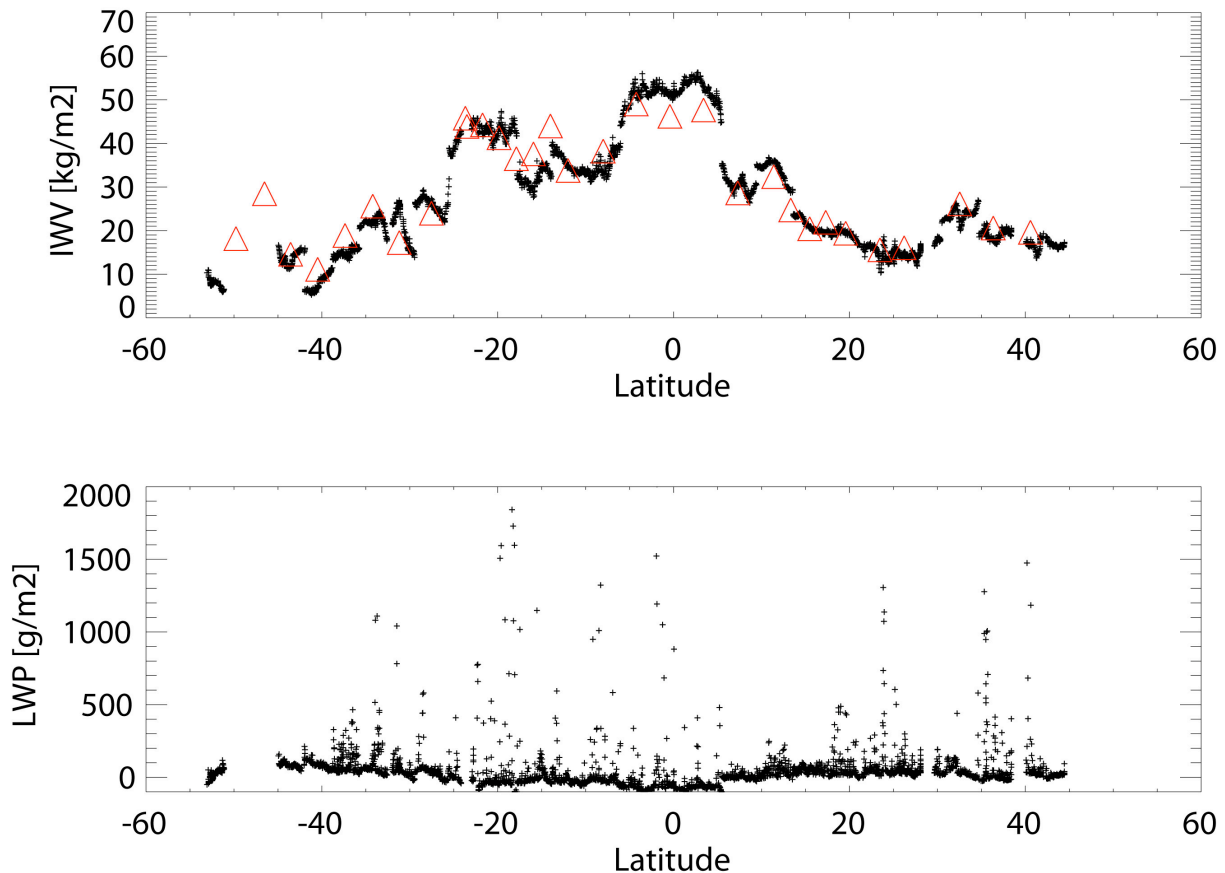
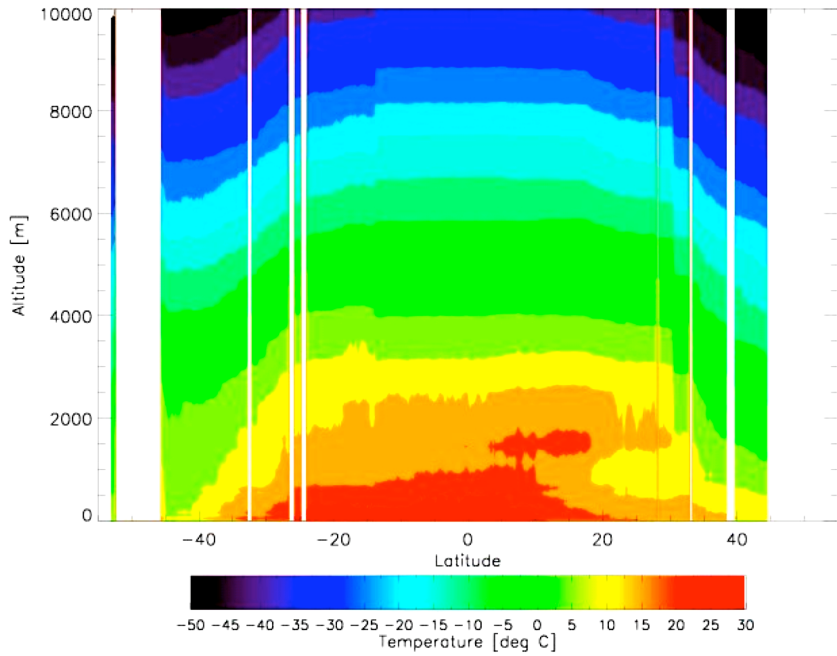
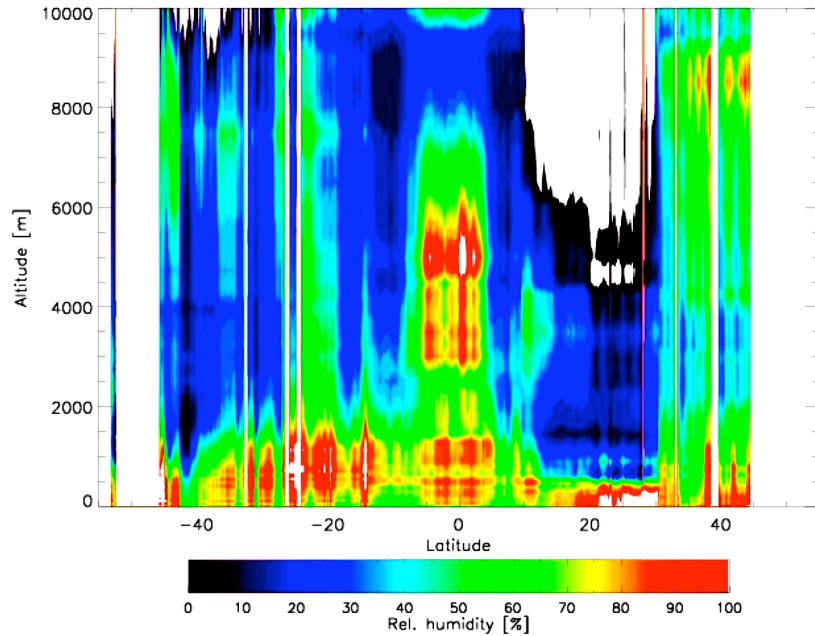


Fig. 4.1: Time series of water vapor path (upper diagram) and liquid water path (lower diagram) from the HATPRO microwave radiometer. The water vapor path from the radio sonde measurements is also shown. Graphics by Bernhard Pospichal

Fig. 4.2 shows the meridional temperature profile along the *Polarstern* cruise. The corresponding humidity profiles are shown in Fig. 4.3. Besides the typical variations caused by the different climate regimes, a Saharan dry air layer advection can be identified around 20 degree north with warmer temperatures and lower humidity values. First comparisons with radiosonde ascents show that the temperature profiles are accurate within 1 – 2 Kelvin, and that large deviations exist for the humidity profiles. The latter is most likely caused by the usage of retrieval algorithms that are not optimized for marine and for tropical/subtropical conditions.



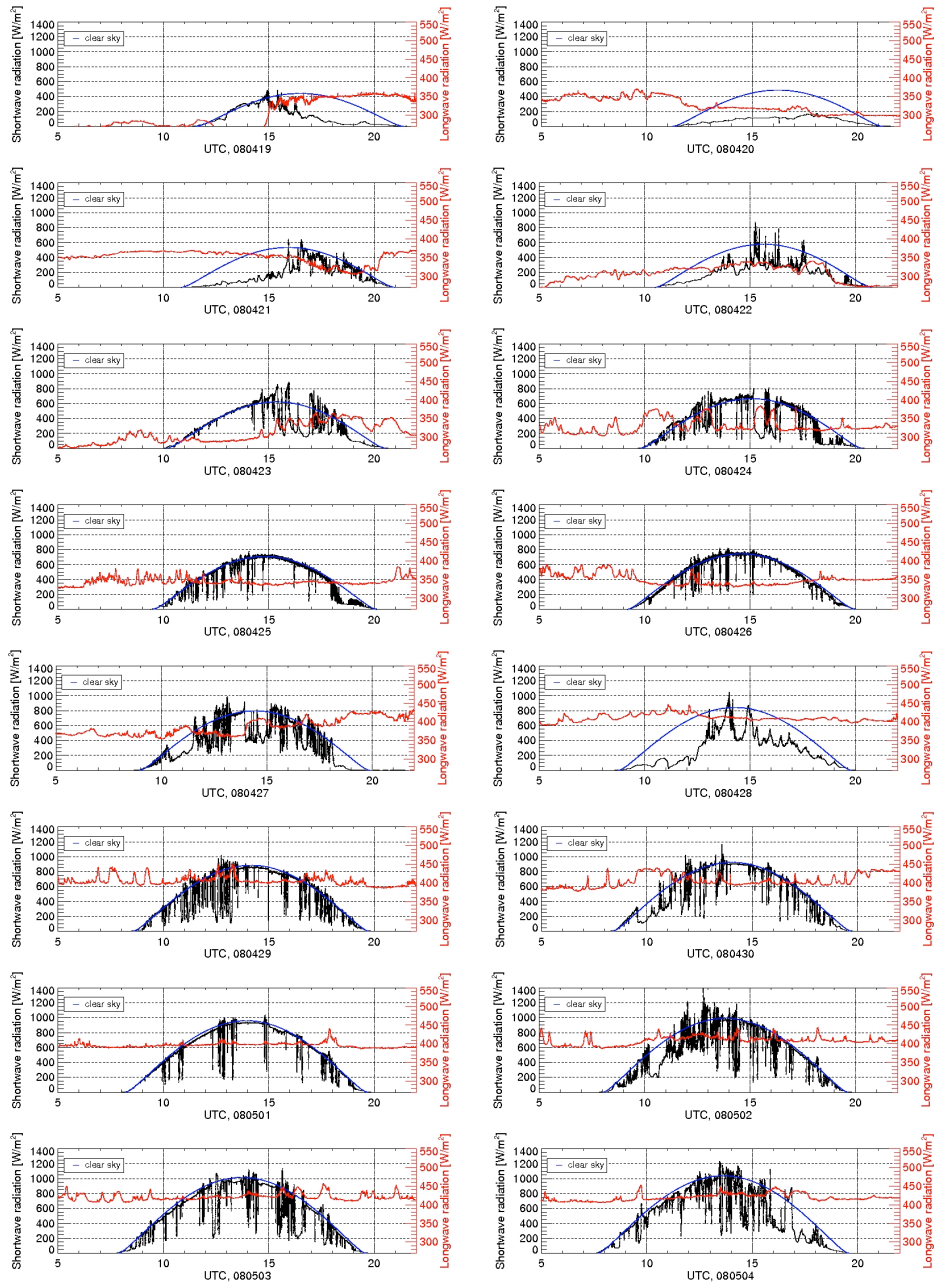
*Fig. 4.2: Vertical profiles of temperature retrieved from the microwave radiometer along the cruise track, shown as a function of latitude. Graphics by Bernhard Pospichal*



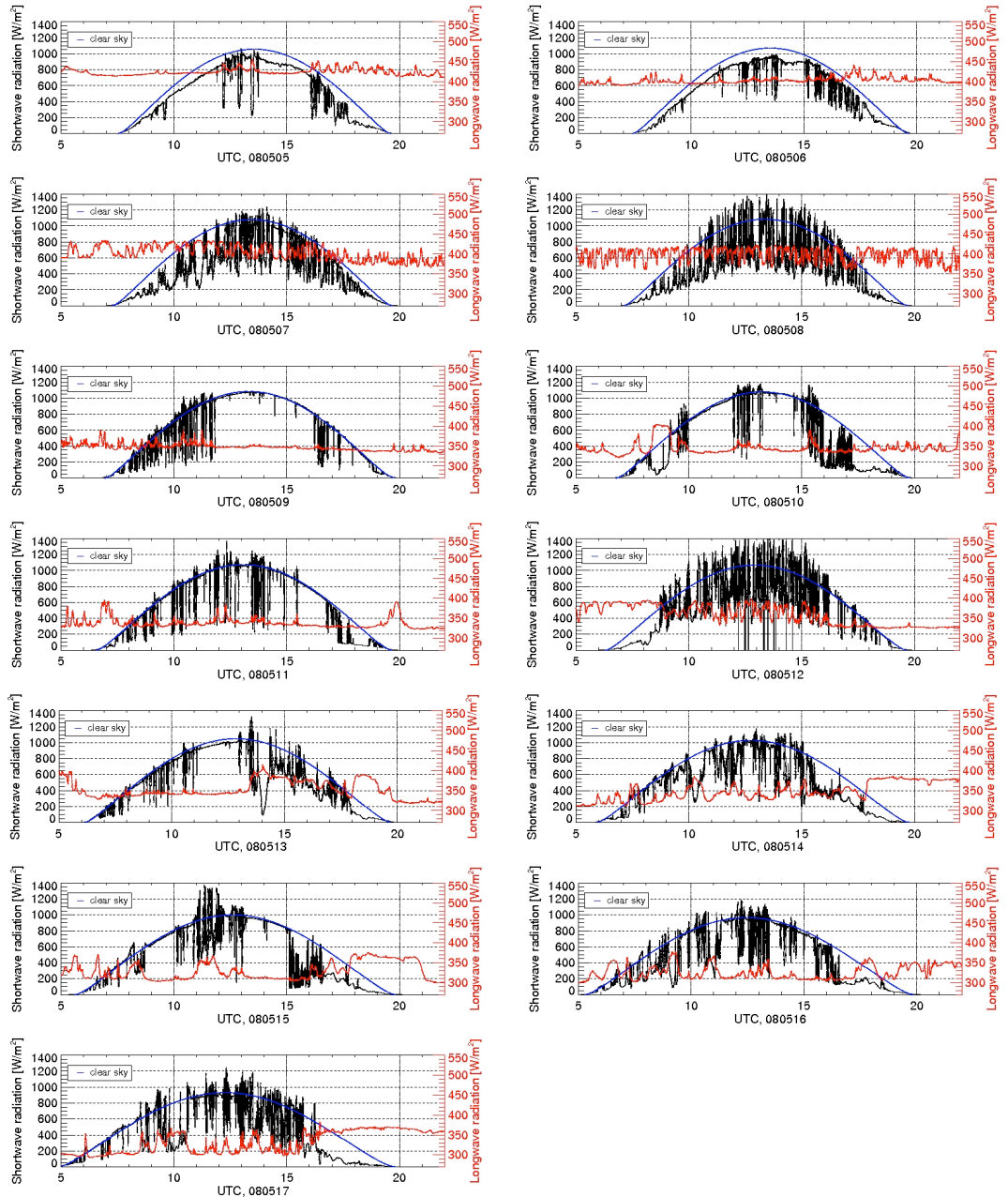
*Fig. 4.3: Vertical profiles of relative humidity retrieved from the microwave radiometer along the cruise track, shown as a function of latitude. Graphics by Bernhard Pospichal*

The daily time series of the downwelling shortwave and longwave radiation along the entire *Polarstern* cruise are summarized in Figs. 4.4(a) and 4.4(b). As a reference, the theoretical curve for clear sky radiation is also shown. Although clouds usually

block the sun and reduce the downwelling solar radiation, many occasions of a radiation excess can be found, which is attributed to the increased diffuse downwelling radiation during broken cloud conditions (because of this termed as “broken cloud effect”). Further analysis will test the correlation between the observed cloud properties like cloud cover and liquid water path, and the surface radiation budget.

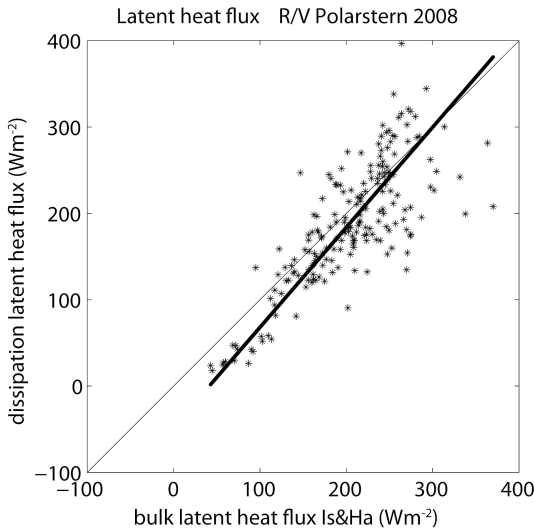


*Fig. 4.4(a): Daily time series of downwelling broadband solar (black) and thermal (red) radiation from April 19 to May 4, 2008. The reference clear sky radiation (blue) is shown for comparison. Graphics by John Kalisch*



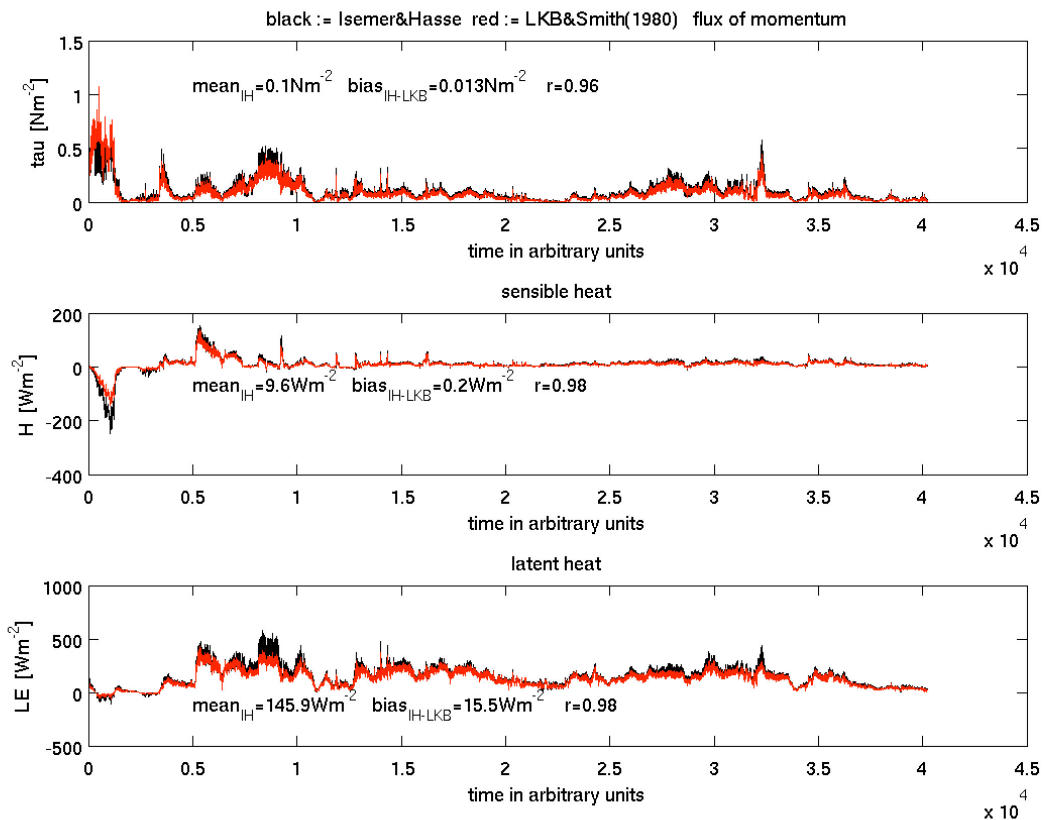
*Fig. 4.4(b): Daily time series of downwelling broadband solar (black) and thermal (red) radiation from May 5 to May 17, 2008. The reference clear sky radiation (blue) is shown for comparison. Graphics by John Kalisch*

A comparison of latent heat flux derived from a combination of a Sonic anemometer and the M100 absorption hygrometer, as well as from a bulk parameterization (Isemer and Hasse, 1987) applied to the ship's meteorological data is shown in Fig. 4.5. It can be seen that bulk parameterization is slightly negatively (positively) biased at small (large) turbulent heat fluxes, and that the differences between both methods increase with increasing heat flux. Further analysis will focus on the specific weather situations that causes the largest uncertainties in the bulk parameterizations.



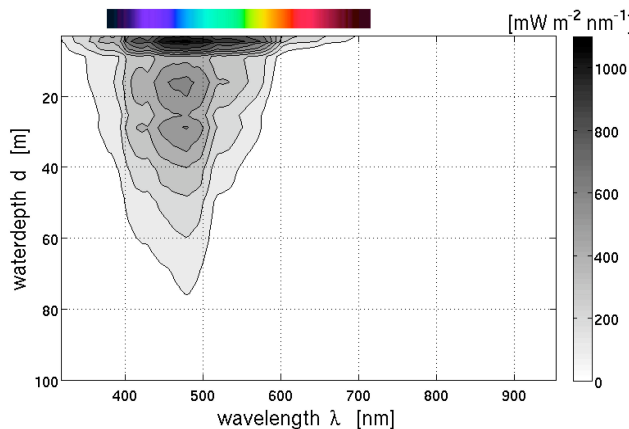
*Fig. 4.5: Latent heat flux based on the dissipation method and from a bulk parameterization*

Figure 4.6 shows a time series of momentum flux, sensible heat and latent heat flux derived from the ships meteorological data applied to the parameterizations from Isemer and Hasse (1987). For comparison the data were also applied to a parameterization by Liu et al. (1979). Obviously, the choice of parameterization is not critical for the derived fluxes.



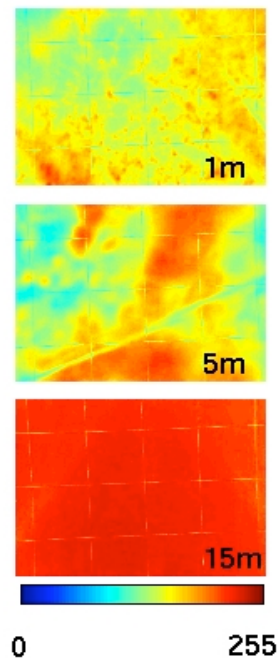
*Fig. 4.6: Time series of two bulk parameterizations of momentum flux, sensible heat flux, and latent heat flux*

Fig. 4.7 shows the mean spectral downwelling subsurface irradiance as a function of depth. Data have been averaged over 1 minute so that surface wave-induced fluctuations are smoothed out. The data show local maxima of irradiance at 15 m and at 30 m depth, probably separately caused by swell and wind sea.



*Fig. 4.7: Mean spectral downwelling subsurface irradiance as a function of depth, measured with the AWI/Uni Bremen RAMSES spectral radiometer. Graphics by Martin Hieronymi*

Examples of typical spatial light fluctuations are shown in Fig. 4.8. It can be seen that the surface wave-induced spatial brightness patterns are very pronounced at low depths and nearly vanish at about 15 m. Note that these pattern are also subject to temporal fluctuations, which are also analysed in this work.



*Fig. 4.8: Normalized brightness fluctuations in the blue spectral region at 1 m, 5 m, and 15 m depth, observed with the IFM-GEOMAR underwater camera system. Graphics by Martin Hieronymi*

## References

- Isemer, H.-J., Hasse, L. (1987) The Bunker Climate Atlas for the North Atlantic Ocean: 2. Air Sea Interactions, Springer, 265 pp
- Liu, H.T., Katsaros, K., Businger, J. (1979) Bulk parameterization of air-sea exchanges of heat and water vapor including molecular constraints at the interface. *J. Atm. Sci.*, **36**, 1722-1735.

---

## **5. AUTONOMOUS MEASUREMENT PLATFORMS FOR ENERGY AND MATERIAL EXCHANGE BETWEEN OCEAN AND ATMOSPHERE (OCEANET) - OCEAN COMPONENT**

Thomas Steinhoff<sup>1)</sup>, Imke Grefe<sup>1)</sup>, Arne Körtzinger<sup>1)</sup>, Martina Gehring<sup>2)</sup>,  
not on board: F. Schroeder<sup>2)</sup>

<sup>1)</sup> IFM-GEOMAR  
<sup>2)</sup> GKSS, Geesthacht

### **Objectives**

This project is part of the WGL-PAKT-Initiative OCEANET which aims to combine the existing expertise of IFM-GEOMAR, GKSS and AWI to further develop, test and install on *Polarstern* autonomous instrumentation for measurement of exchange of energy and matter between the atmosphere and the surface ocean. The long term goal of this initiative is to provide operational approaches for unattended operation on “Voluntary Observing Ships”.

The oceanic component of this study focuses on the marine carbon cycle in the surface ocean which is of high climate relevance but at the same time susceptible to climate change. The surface ocean’s CO<sub>2</sub> source/sink function is maintained by a complex interaction of physical and biological processes. A deconvolution of these driving forces requires both a rather comprehensive observational approach as well as high spatial and temporal coverage. These requirements can only be met with multi-parameter observational approaches that can be operated in unattended mode on platforms such as merchant vessels.

During this first OCEANET cruise the feasibility of autonomous underway measurements was assessed for a wide range of instruments for measurement of physical (temperature, salinity, turbidity), chemical (CO<sub>2</sub> partial pressure, pH, oxygen, total gas tension, nutrients), and biological parameters (chlorophyll a, photosynthetic parameters).

### **Work at sea**

During ANT-XXIV/4 we operated several underway instruments in the wet laboratory of *Polarstern*. A centerpiece of this suite of underway systems was the FerryBox system (4H-Jena Engineering GmbH) by which autonomous underway measurements of temperature and salinity, turbidity, chlorophyll a fluorescence, dissolved oxygen, and pH were carried out. The data was stored along with time and geographical position at 1-min intervals. Additionally, two nutrient analyzers for dissolved nitrate and phosphate were operated on the continuous seawater supply system. Finally, a new sensor for variable chlorophyll-a measurement (Phytoflash,

Turner Designs) to determine the quantum efficiency of phytoplankton as a measure of its physiological status was tested during this cruise.

A second centerpiece of the ocean component of OCEANET was the comparison of as many instruments for the measurement of the CO<sub>2</sub> partial pressure (*p*CO<sub>2</sub>) in seawater as possible. Unfortunately three out of the six *p*CO<sub>2</sub> systems to be operated in parallel were stuck in customs in Santiago de Chile and did not meet the ship in Punta Arenas. These systems will therefore be used in the follow-up experiment during ANT XXIV/1 in Nov. 2008. The following three systems were successfully operated throughout the cruise.

### **General Oceanics Underway pCO<sub>2</sub> System (GO)**

The gas phase is equilibrated with seawater using a spray-head equilibrator that produces a fine spray. After the equilibration process the sample gas is dried and subsequently measured via NDIR using a LICOR 7000 gas analyzer. The LICOR is calibrated approximately every 3 hours with 3 standard gases ranging from 174 to 734 ppmv.

### **SPRINK Underway pCO<sub>2</sub> System (SPRINK)**

The principle of measurement is the same as for the GO system with the exception that the equilibration is performed in a combined “bubble-type” and “laminar-flow” equilibrator. Again the gas is dried after equilibration and measured by means of an NDIR detector (LICOR 6252) that is calibrated as mentioned above. A detailed description of the instrument is given in Körtzinger et al. (1996).

### **PSI CO<sub>2</sub> Pro pCO<sub>2</sub> Sensor (PSI)**

In this autonomous *in-situ* sensor, the CO<sub>2</sub> in a gas phase is equilibrated with the seawater via a tubular silicone membrane. The CO<sub>2</sub> in the gas phase is measured via a small NDIR cell that is calibrated every 3 - 24 h by a simply a zero-point calibration.

Fig. 5.1 shows the scheme of the setup of the instruments. The SPRINK and GO systems were connected directly to ship's seawater supply line which drew seawater from around 11 m depth. Temperature and salinity were measured directly at the seawater intake by the shipborne thermosalinograph. The PSI sensor, in contrast, was submerged into a thermally insulated flow-through water bath that was also connected to the seawater supply line. The containers water volume was 40 l and the water flow through it was maintained at approximately 13 l/min. In addition we submerged an oxygen optode sensor (Aanderaa, Norway) as well as a gas tension device (GTD Pro, Pro Oceanus, Halifax, Canada) in the flow-through container. The latter measures the total pressure of all dissolved gases in the seawater. After several problems with the GO system, the first quality data of this system were acquired north of 35°S. Unfortunately a pump that supplies water to the gas tension device broke only a few days after departure from Punta Arenas, so that no parallel gas tension data measurement were possible after that.

For reference, discrete samples for dissolved inorganic carbon (DIC) and total alkalinity (TA) were taken every 6 hours for analysis at the IFM-GEOMAR in Kiel. The samples were drawn into 500 ml bottles and poisoned with saturated mercuric chloride solution.

Finally, filtration of surface seawater from approx. 11 m depth was performed every 8 hours. These samples are being screened at the IFM-GEOMAR in Kiel for the genetic sequence of the enzyme nitrogenase. This enzyme mediates the reduction of molecular nitrogen to ammonia.

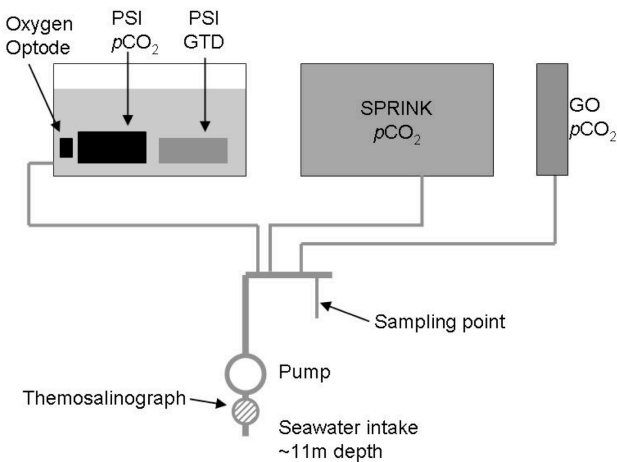


*Fig. 5.1: Setup of underway pCO<sub>2</sub> instruments during cruise ANT-XXIV/4 of Polarstern*

### Preliminary results

The CO<sub>2</sub> mole fraction (xCO<sub>2</sub>) data as recorded by the SPRINK and the GO system were calibrated against the standard gases and together with the atmospheric pressure and the sea surface temperature the sea surface pCO<sub>2</sub> was calculated following the procedures described in Dickson et al. (2007).

The combined patterns of pCO<sub>2</sub> (Fig. 5.2) and dissolved oxygen (Fig. 5.3) along the cruise track can be interpreted in terms of the driving forces of which the seasonal cycles of sea surface temperature and net community production are the most important ones. Their effect on surface disequilibria of CO<sub>2</sub> and O<sub>2</sub> is very different owing to the two gases very different air-sea equilibration times scales (roughly 1 years vs. 1 month). The observed general patterns of CO<sub>2</sub> supersaturation in subtropical waters and undersaturation associated with elevated biological productivity at the equator and in subpolar waters is in agreement with the climatological picture (Takahashi et al., 2002). Oxygen deviations from the equilibrium therefore indicate ongoing or recent processes an example of which is a patch of fresh upwelled waters off northwest Africa encountered around 20°N. pCO<sub>2</sub> data calculated from the discrete samples of DIC and TA (Fig. 5.2) serve as an independent quality control.

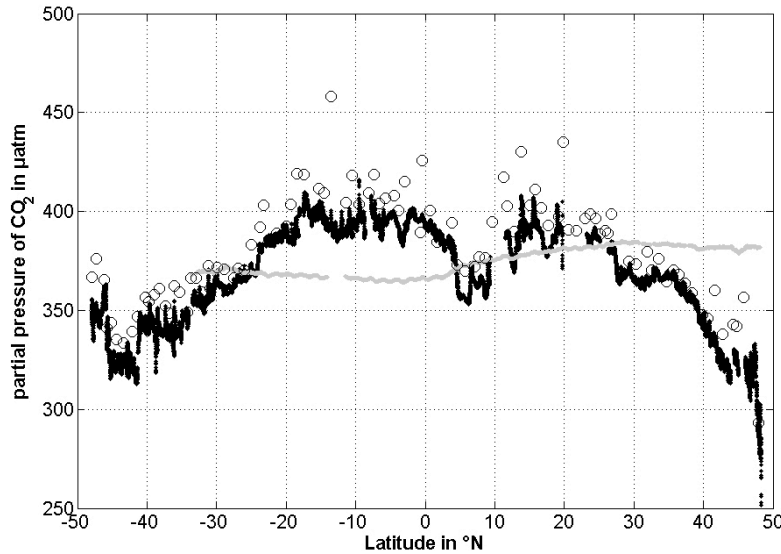


Fig. 5.2: Surface ocean (black dots) and atmospheric (grey line)  $p\text{CO}_2$  as measured during cruise ANT-XXIV/4 of Polarstern. The open circles denote  $p\text{CO}_2$  data that were calculated from the discrete measurements of DIC and total alkalinity using the appropriate thermodynamic relationships.

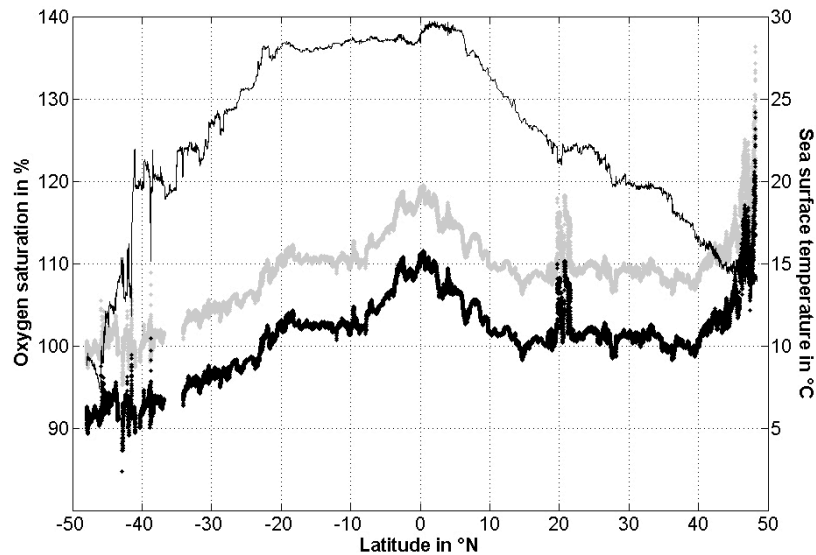


Fig. 5.3: Raw oxygen saturation (grey dots) and sea surface temperature (thin black line) as measured during cruise ANT-XXIV/4 of Polarstern. Oxygen data have not been finally calibrated but appear to be high by about 8 %. Black dots show oxygen saturation corrected by 8 % which is close to the final calibration result.

A comparison of the  $p\text{CO}_2$  data of the three instruments is shown in Fig. 5.4. As mentioned above, all seawater  $p\text{CO}_2$  data have been corrected to *in-situ* seawater temperature. We used the GO system as our reference system as this is the most

intensively tested and internationally accepted instrument. Except for two peaks between 8°S and 20°S, the mean difference between the SPRINK and the GO systems is reasonably small at 2 - 3  $\mu\text{atm}$ . Some of this disagreement is probably due to slight differences in the calibration of the temperature probes used to measure the temperature of equilibration. This difference will be taken care of by post calibration. The two peaks in the SPRING-GO  $p\text{CO}_2$  difference may be due to a drop in the water flow rate as well as problems with condensation in the of the SPRINK system. The more reliable design and measurement concept of the GO system avoid and also detect the occurrence of such unfavorable conditions.

The difference between the PSI and GO systems is more variable which can be explained by the very different design of the PSI sensor which as an autonomous submersible sensor cannot achieve the accuracy levels of the GO and SPRINK system. Some of the deviations can probably be explained by fouling of the PSI sensor's membrane which to some extent disappeared after cleaning the membrane with acid. Some of the deviation is clearly also due to the characteristics of the PSI sensor which has a very long time constant of about 20 minutes as compared to the 1 - 2 min of the GO system. The results also point at problems arising from disequilibria in the gas matrix (i.e. oxygen and humidity) which can lead to transient pressure changes and hence changes in the composition of the equilibrated gas phase that do not represent ambient  $p\text{CO}_2$  conditions. Full exploration of the large  $p\text{CO}_2$  data set will allow to assess consequences of such limitations in the light of the PSI sensor's suitability for autonomous use on "Voluntary Observing Ships".

The evaluation of the entire dataset is currently underway at the IFM-GEOMAR and GKSS.

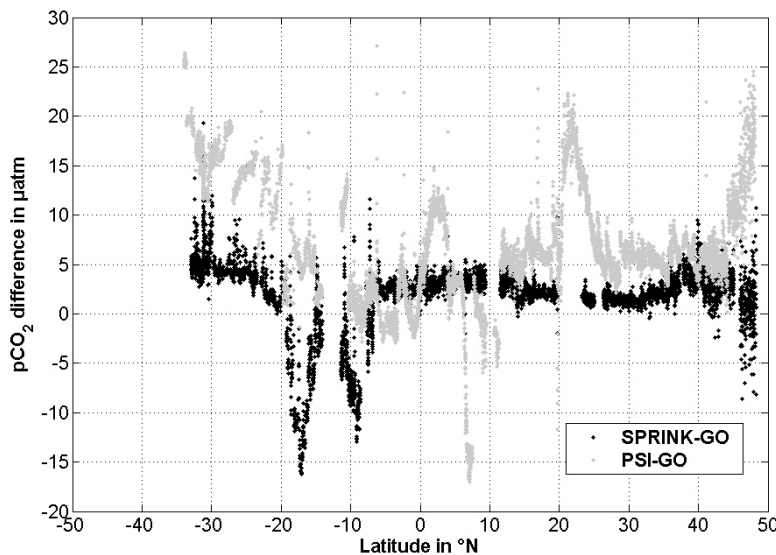


*Fig. 5.4: Difference in the measured  $p\text{CO}_2$  between SPRINK and GO system (black dots) and PSI and GO systems (grey dots), respectively*

## **References**

- Dickson, A.G., Sabine, C.L., Christian, J.R. (Eds.) (2007) *Guide to Best Practices for Ocean CO<sub>2</sub> Measurements*. PICES Special Publication 3.
- Körtzinger, A., Thomas, H., Schneider, B., Gronau, N., Mintrop, L., Duinker, J.D. (1996) At-sea intercomparison of two newly designed underway pCO<sub>2</sub> systems - encouraging results. *Mar. Chem.*, **52**, 133-145.
- Takahashi, T., J. Olafson, J. G. Goddard, D. W. Chipman, and S. C. Sutherland. 1993. Seasonal Variation of CO<sub>2</sub> and Nutrients in the High-Latitude Surface Oceans: a Comparative Study. *Global Biochem. Cycles*, **7**, 843-878.

---

## 6. AEROSOLS

Stefan Kinne  
MPI-Met

### Objectives

There are always aerosol particles in our atmosphere. Aerosol particles originate from different natural and anthropogenic sources. Besides its direct effects on the radiation budget aerosol is a controlling factor in cloud particle formation and growth, in turn affecting cloud reflectivity (of sun-light), cloud lifetime and subsequent precipitation processes. To develop trust in offered aerosol data-sets, agreement to quality data needs to be demonstrated. For aerosol, these quality references can be provided by ground-based remote sensing. Remote sensing from ground has the advantage over remote sensing from space that measurements of the attenuation of direct sun-light provide a solid measure for the aerosol amount and even estimates for aerosol size.

### Work at sea

To build up data on aerosol properties (aerosol optical depth [AOD] for aerosol amount and AOD solar spectral dependence for aerosol size estimates) handheld MICROTOPS sun-photometer and GPS instruments are distributed to ship-passengers on an opportunity basis. The concept of the MICROTOPS sun-photometer is rather simple. UTC time and GPS location determine how much solar energy can be expected. The measured sun-light provides information by how much the aerosol has attenuated the direct sun-light. This sun-light sampling is done at specific solar sub-spectral regions (e.g. at 440 nm, at 500 nm, at 675 nm and at 870 nm) to avoid interference by trace-gas absorption. The challenge in operating the instrument is to find cloud (an especially cirrus) free views of the sun and to point the instrument during sampling directly into the sun, with the help of a visual device on top of the instrument.

### Preliminary results

Fig. 6.1 demonstrates the rather low aerosol loading over the Atlantic of the Southern Hemisphere. AOD values are usually lower than 0.15 and at times even as low as 0.05. Only regions impacted by advection of continental air from South America (between -35° to -25° S) and from Africa (north of 5° S) show larger background AOD values in the Southern Atlantic.

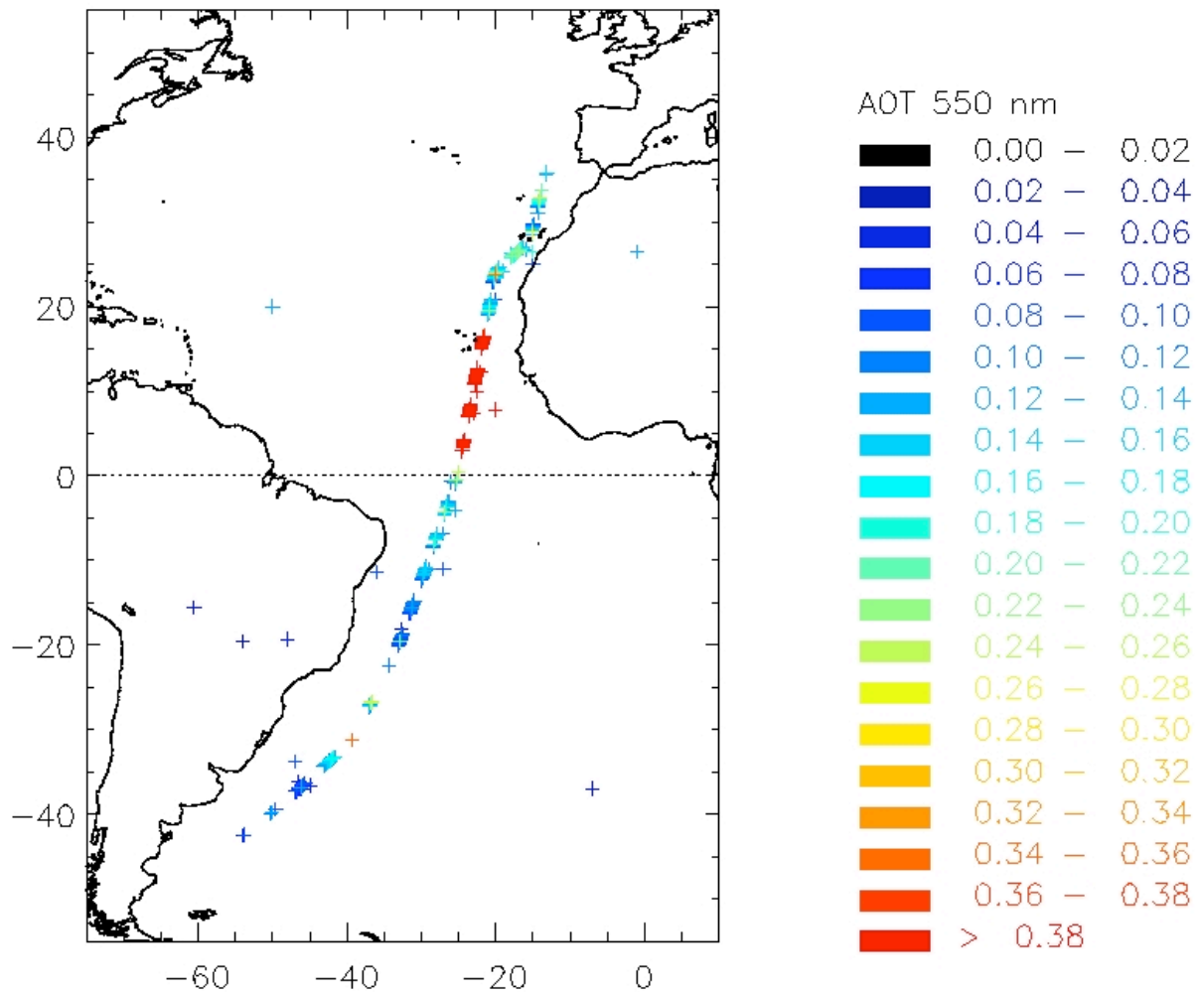
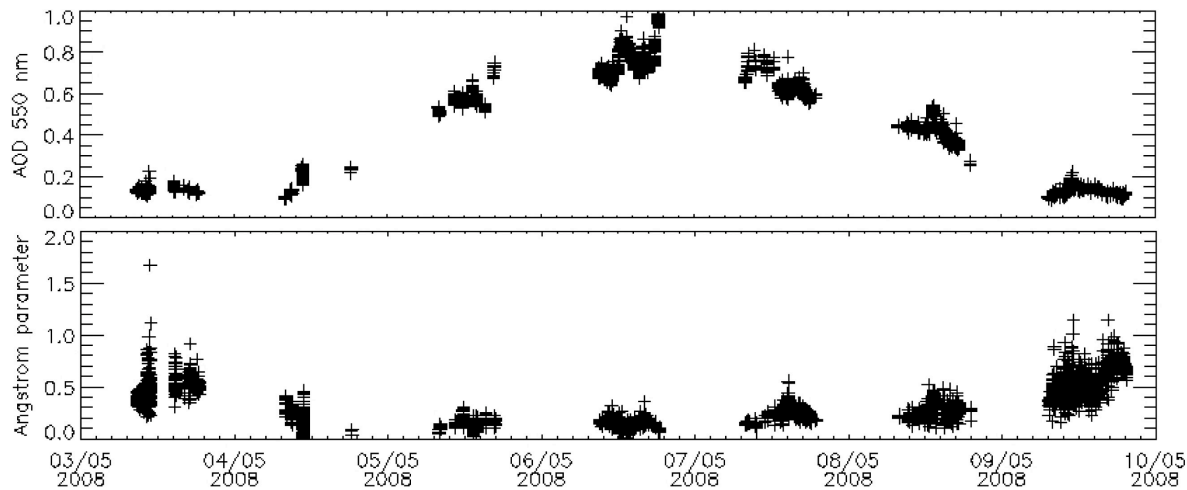


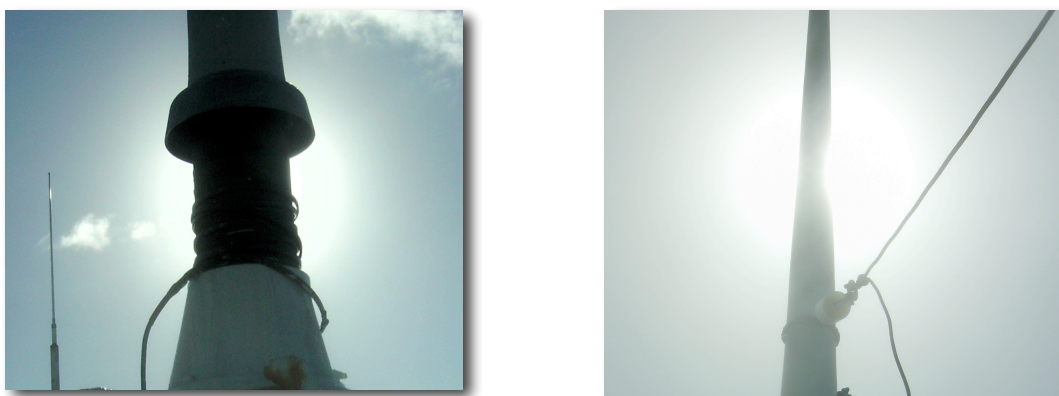
Fig. 6.1: Sampled aerosol optical depth over the Atlantic. Graphics by Bernhard Pospichal

Fig. 6.1 also shows that after passing the equator (and shortly after that the ITCZ) the AOD dramatically increased as an airmass with dust-loading from the Saharan desert was encountered. Fig. 6.2 illustrates the temporal development of the AOD and of the Angstrom parameter. This parameter is defined on the AOD spectral dependence to provide information about aerosol size, as if aerosol particles get smaller the Angstrom parameter increases.



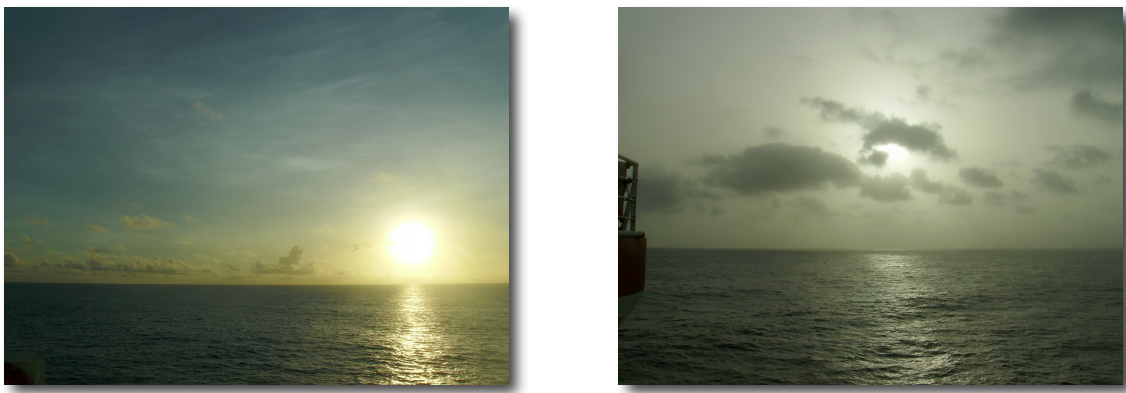
*Fig. 6.2: Time-series of mid-visible AOD and Angstrom parameter during the dust event*

During the dust event the size of the aerosol increased as the Angstrom parameter dropped below 0.4. The sampled mid-visible optical depth reached maximum values of almost 1 during May 6 and May 7. There is confidence that the data on May 7, 8 and 9 refer to aerosol only, whereas on the initial 3 days (May 4, 5 and 6) cirrus clouds at times could have exaggerated the dust signal. Cirrus contaminations can be expected at periods when the Angstrom parameter falls below 0.1, because large ice-crystals have basically no solar spectral dependence (Angstrom of zero) and dust being further away from dust has Angstrom parameters between 0.2 and 0.5, as demonstrated on the only aerosol days of May 7 and 8.



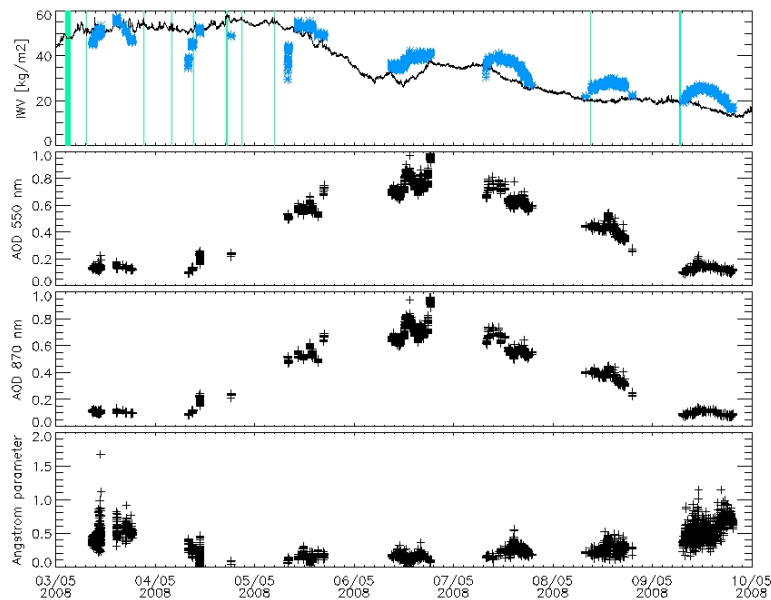
*Fig. 6.3: Under cloud-free conditions the dust enhanced background (right) displays the image of the sun in a much more diffuse image than for maritime background (left).  
Photo by Stefan Kinne*

Fig. 6.3 compares the shape of the sun's disk, which is rather diffuse in appearance under enhanced dust conditions. Fig. 6.4 compares views of sunrise and sunset. With dust the entire sky has a much whiter and also less colorful appearance (as dust particles more attend more evenly all colors of the visible sun-light than marine background aerosol).



*Fig. 6.4: Sunrise at maritime background (May 04) and sunrise with added dust (May 7). Photo by Stefan Kinne*

A time-series of MICROTOPS data is given of the AOD at 870 nm for the Angstrom parameter (based on AODs at 500 nm and 870 nm), an estimate for the AOD at 550 nm (a reference wave length in modelling) and the derived atmospheric water vapor. The water vapor data, involving solar attenuations at 936 nm (a spectral region where water vapor absorbs) compare well with independent measurements by the microwave radiometer instrument. Only during noon (when the air-mass factor is relatively small) the MICROTOPS seem to overestimate atmospheric water.



*Fig. 6.5: Time-series of MICROTOPS data for the Saharan dust event: total water vapor (top panel, comparison to microwave data), AODs at 550 and 870 nm (center panels) and Angstrom parameter (lower panel). The top panel shows a comparison to water vapor data of a microwave instrument. Graphics by Bernhard Pospichal*

## 7. ADCP MEASUREMENTS

P. Brandt (not on board)  
IFM-GEOMAR

### Work at sea

During ANT-XXIV/4 current velocity measurements were carried out using the shipboard 150 kHz Ocean Surveyor ADCP. Data were acquired from 22 April to 17 May 2008. The equatorial current system was crossed at about 26°W.

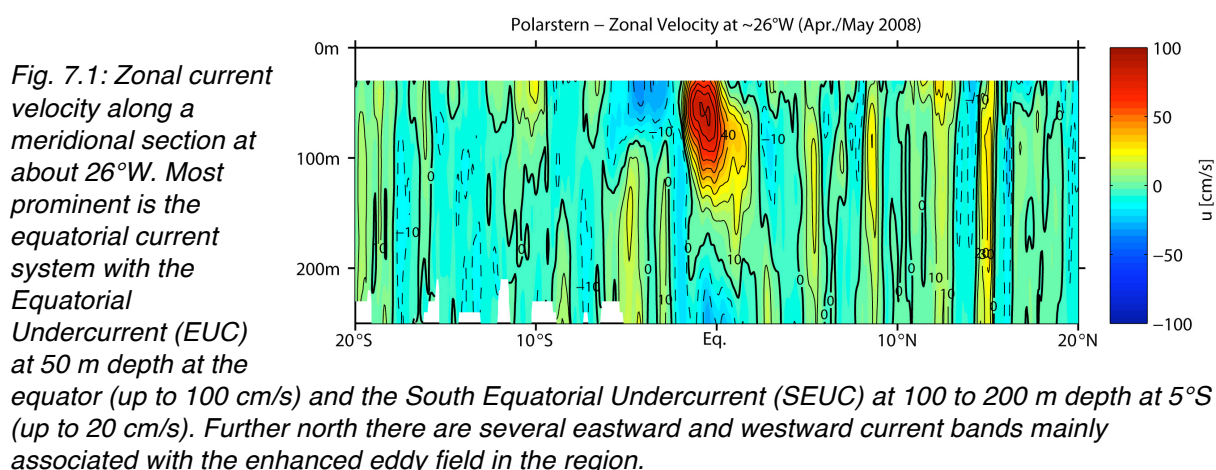
### Preliminary results

The velocity data obtained after processing are of good quality. Depth range is 200 to 250 m for the whole cruise. Thanks to frequent purposeful deviations from a straight cruise track, the transducer misalignment - which is an essential factor in data processing - could be determined quite well. Those purposeful deviations prove most suitable if the time intervals between course changes are 10 minutes at least and course changes are 10 degrees at least. Heading data were utilized from the Laser-navigation-platform. This heading resulted in slightly lower data quality compared to a previous cruise in 2005 (ANT-XXII/5) when the heading from the ASHTECH array was also available. The obtained uncertainty in the calculated transducer misalignment was 0.5 degrees compared to 0.3 degrees if the heading from the ASHTECH array was applied.

These data have been used in the following studies:

Fischer, J., Hormann, V., Brandt, P., Schott, F.A., Rabe, B., Funk, A. (2008), The South Equatorial Undercurrent in the western to central tropical Atlantic, *Geophys. Res. Lett.*, doi:10.1029/2008GL035753, in press.

Hormann, V. (2008) *Upper equatorial Atlantic circulation and cold tongue variability*. Ph.D. thesis, IFM-GEOMAR, Kiel, Germany.



---

## **8. FINAL SEA TRIAL AND CALIBRATION OF THE ATLAS HYDROSWEEP MULTIBEAM ECHOSOUNDER DURING ANT-XXIX/4, LAS PALMAS - BREMERHAVEN (12.05.2008 - 20.05.2008)**

Fred Niederjasper<sup>1)</sup>, Saad El Naggar<sup>1)</sup>,  
Thomas Liebe<sup>2)</sup>, Martin Boche<sup>2)</sup>

<sup>1)</sup> Alfred-Wegener-Institute, Bremerhaven

<sup>2)</sup> Reederei F. Laeisz (Bremerhaven)

### **History and description**

Hydrosweep is a multibeam sonar, which transmits and receives acoustic waves of 15.5 kHz frequency within a fan of 90° to 120° opening angle athwart ship and 2° opening angle along the ship. The travel times of the reflections from the sea floor, combined with the sound velocity (profile) of the water column, are used to derive high-resolution bathymetric maps which reveal the topography of the ocean floor in great detail. The amplitudes of the reflections from the sea floor, sampled by 2000 points along the swath, simultaneously provide Side Scan Sonar images which indicate high and low scattering areas on the sea floor by light and dark gray-shaded colours. The currently installed Hydrosweep DS-2 system includes an upgrade which allows (1) to use 240 "soft" beams (HDBE Mode = High Definition Bearing Estimation Mode) instead of the conventional 59 "hard" beams of the former system versions for high-resolution bathymetric surveys and (2) to reduce the source level manually and automatically (ASLC mode = Automatic Source Level Control Mode). A correctly working HDBE mode is mandatory for an application of the ASLC mode. Three different settings can be used to control the source level: (1) Standard, (2) Maximum Source Level, (3) Automatic Source Level Control (ASLC).

### **Standard Source Level control**

In case of a "Standard Source Level control" the system is running in the high-resolution HDBE mode with a maximum constant source level of 239 dB in the deep sea, an operator-defined coverage of the transmission and receiver swaths of 90° to 120°, a "Start Time Variable Gain" (Start TVG) set by the operator, and an automatically determined "Actual Time Variable Gain" (Actual TVG) optimized according to the level of the received data.

### **Maximum Source Level**

In case of a "Maximum Source Level" control the transmitted source level and the transmission and receiver swath widths are defined manually by the operator. The time variable gain can either be determined automatically or manually. In case of an automatic gain control the "Start TVG" is set by the operator and the "Actual TVG" is optimized within a range of ±12 dB according to the computed S/N ratio of the

received data. Ideally, a value of 18 dB is chosen for the "Start TVG" so that a maximum gain of 30 dB can be reached. In case of a manual gain control both "Start TVG" and "Actual TVG" are set manually to the same constant value, maximum to 18 dB. If the maximum source level and the (manually defined) gain are chosen too low, the outer beams of the swath might become unusable.

### **Automatic Source Level Control (ASLC)**

In case of an "Automatic Source Level Control (ASLC)" the system tries to optimize and reduce the source level automatically so that operator-defined values for the maximum source level, the receiver swath width and the S/N ratio of the received data are fulfilled. This is reached by decreasing the transmission source level and increasing the "Actual TVG" simultaneously such that the computed S/N-ratio and the desired coverage of the received data is higher than or equal to the operator-defined value. Again, a "Start TVG" of maximum 18 dB can be chosen by the operator, whereas the "Actual TVG" is varied automatically by  $\pm 12$  dB.

### **Objectives**

A major maintenance was carried out on all transducers of the Hydrosweep during the shipyards' stay of *Polarstern* in May 2007 in Bremerhaven. The hull mountings' kits were replaced by a new stainless steel.

All transducers wiring were disconnected and reconnected after the installation to the system. Finally a system check was carried out by Atlas Hydrographic.

During ARK-XXII/1 cruise a second system check on real operation conditions was carried out by scientists and Atlas Hydrographic. All system checks and data analysis confirmed the proper function of the Hydrosweep.

During ARK-XXII/2 cruise the system was used by scientists for ordinary bathymetric survey. Data analysis at AWI shows that the system was not operating properly, because systematic errors were found in the collected and analysed data. The hardware including transducer was checked again by Atlas Hydrographic in Punta Arenas on 18.04.08.

During the last part of the cruise ANT-XXIV/4 (Las Palmas – Bremerhaven, 12.05.2008 – 20.05.2008) a final system check, sea trial and calibration were carried out by AWI's scientists. Data analysis shows that the system is now operational and can be used for bathymetric survey and research.

---

## **9. SEA TRIAL AND TESTING OF THE NEW UPGRADED DEEP SEA SEDIMENT ECHO SOUNDER “PARASOUND DS III-P70” DURING ANT-XXIV/4 (THIRD PHASE)**

Frank Niessen<sup>1)</sup>, Saad El Naggar<sup>1)</sup>,  
Thomas Liebe<sup>2)</sup>, Martin Boche<sup>2)</sup>, J.  
Ewert<sup>3)</sup>

<sup>1)</sup> Alfred-Wegener-Institute, Bremerhaven,

<sup>2)</sup> Reederei F. Laeisz (Bremerhaven),

<sup>3)</sup> Atlas Hydrographic GmbH (Bremen)

### **Overview of previous sea-trial and testing on *Polarstern* in 2007**

The Deep Sea Sediment Echo Sounder “PARASOUND DS III-P70” (ATLAS HYDROGRAPHIC, Bremen, Germany) was upgraded from DS II to DS III-P70 during the shipyards stay of *Polarstern* in Bremerhaven between 04.05.07 and 29.05.07. This upgrade included a complete installation of new hardware and software, of which this report describes the third sea-trial phase including final software updating and testing at sea. An overview about the basic system set up is given in (Klages & Thiede in prep.). A brief description of additional options offered by DS III-P70 including data examples and a comparison with data from the previous system DS II on *Polarstern* is given by Niessen et al. (in Schiel in prep.).

The first operational test under real conditions at sea was carried out during the first part of the cruise ARK-XXII/1 between Bremerhaven and Tromsø from 29.05.07 until 06.06.07 (Klages & Thiede in prep.). Basic functions were tested and malfunctions listed. An extensive deep-water test of the system (> 3,000 m) was not carried out due to the lack of sufficient deep-water environment along the cruise track.

The second (and originally planned as final) sea trial was carried out during the cruise ANT-XXIV/1 on route from Bremerhaven to Las Palmas (26.10.07 to 03.11.07), where deep-sea conditions with more than 4,000 m allowed running a broader range of operational settings (Schiel 2008 in prep.). During this leg the system was brought up to nearly fault-free functions of all possible settings with only a few problems remaining. The latter included incorrect distance plots and uncertainties with respect to negative influence of ships motion on data acquisition. However, the system was not used under full expedition conditions thereafter because the remaining legs of ANT-XXII did not include geosciences projects.

Meanwhile in 2008, various system problems were reported from other research vessels while operating with DS III-P70 including RV *Meteor* and RV *Maria S. Merian*. This has led to improvements of software modules on-route of these ships and at ATLAS HYDROGRAPHIC, Bremen, Germany. Consequently, and as a result of recent software-module releases, AWI, Reederei F. Laeisz and ATLAS HYDROGRAPHIC decided to update the system and to carry out a third and final

sea-trial and test phase of DS III-P70 on *Polarstern* during the last part of the leg ANT-XXIV/4 on route from Las Palmas to Bremerhaven (12.05.2008 – 20.05.2008).

## **Objectives**

One of the objectives of the third sea trial of DS III-P70 was to ensure that the latest software versions of the control modules are installed on *Polarstern* in order to have equal systems on all three German vessels where DS III-P70 is used. The other goal was to provide a tested and fully functional system for the forthcoming cruise leg ARK-XXIII/3 during which Parasound data is needed for the geosciences projects.

The work at sea had several goals:

- Completion and tuning of the final installation.
- Operational checks according to the list of faults formulated during the second sea trial tests on ANT-XXIV/1.
- Operational checks on all system functions, where problems were reported from other vessels.
- Performance of a 48 hour system-stability test while simulating real-time expedition conditions for system operation.
- Backing-up and system preparation for the forthcoming leg ARK-XXIII/3.

## **Work at sea**

The cruise time from Las Palmas to Bremerhaven was used to install the improved software components of the DS III-P70 system. Whenever possible, the system was run in continuous (24-hour) operation to test general system stability and correct operation in both operator-controlled and automatic modes of operation. Two previous problems observed during the second sea-trial on ANT-XXIV/1 were analyzed and a 48-hour stability test was carried out.

Distance bars on all data outputs (on-line profile on screen and print (ASD-Files), replay plots from PS3-Files) had in common that lateral distances were too long by a factor of up to two. The analysis of trace-header data of both PS3- and SEG-Y-Files revealed arbitrary jumps in GPS positions leading to calculated distances longer than real. After further analysis it was found that a terminal server of the ship's data distributing system (MINS) had malfunction leading to time delay in transmission of navigation data to the DS III-P70 system by up to 8 seconds. As a result, Parasound received a mixture of correct and incorrect (previous) navigation data causing partly faulty positions for correctly measured Parasound traces. After the problem was fixed, all DS III-P70 system-data output was positively checked for correct distance plotting and trace-header data.

After having fixed previous problems of not fully compensated ships motion (roll, heave and pitch) to Parasound transmission and reception, the result could not finally be tested during sea-trial phase two. Thus, ship motion experiments were carried out in the Bay of Biscay at more than 4,000 m water depth, where roll angles of up to

+/ 3° were reached. There was no effect of roll motion observed in Parasound PHF and SLF data output. Effects of pitch and heave could not be tested as the sea was calm during the entire journey and these motion effects cannot be simulated.

During a 48 hour test with expedition type of data acquisition (watch-keeping and running the system with all necessary modes and adjustments) system operation using Hydromap Control and Parastore remained functioning in a depth range from more than 4,000 m to 100 m and different bottom topography, penetration and back-scatter conditions. This test was carried out from the continental slope northwest of Spain near Vigo across the Bay of Biscay onto the continental shelf west of France near Brest.

The remaining time, operation in different modes such as single-pulse transmission, quasi-equidistant transmission and pulse train were tested under different boundary conditions and different depth control. The system was then backed up and prepared for settings to be used during the next geosciences' leg ARK-XXIII/3 in 2008. During the entire work period the system was operated for test purposes only including data acquisition, which was purely used to check data accuracy and quality and not for any kind of research or other use. No data were stored and taken off the vessel for later examination.

## Conclusions

After intensive testing of diverse modes and functions using the latest software-component update of the DS III-P70 system on board *Polarstern*, we found the system fully functional, producing high quality and correct data as needed for polar marine geosciences in forthcoming expeditions. We were not able to analyze effects of ships motion (pitch and heave > 0.5 m) on both sound transmission and sound reception as these ship motions did not occur during our testing phase.

## References

- Klages M. & Thiede J. (in prep.).- The expeditions ARKTIS-XXII/1a-c of the research vessel *Polarstern* in 2007 / Ed. by Michael Klages and Jörn Thiede with contributions of the participants. Reports on Polar and Marine Research
- Schiel S. (in prep.).- The expeditions ANTARKTIS-XXIV/1 of the research vessel *Polarstern* in 2007 / Ed. by Sigrid Schiel with contributions of the participants. Reports on Polar and Marine Research

---

## **10. SATELLITE GROUND TRUTH: BIO-OPTICAL AND ATMOSPHERIC STUDIES**

Bettina Schmitt<sup>1)</sup>, Laila Bentama<sup>2)</sup>, Anja Theis<sup>3)</sup>, Hagen Schulte in den Bäumen<sup>3)</sup>, Marc Taylor<sup>1)</sup>

<sup>1)</sup>Alfred-Wegener-Institute, Bremerhaven

<sup>2)</sup>GKSS, Geesthacht

<sup>3)</sup>IUP, Institute of Environmental Physics,  
University of Bremen

### **10.1 Bio-optical measurements**

#### **Objectives**

It has been estimated that marine phytoplankton contributes 30 to 60 % to global primary production. The large uncertainty range is a result of the lack of global information on phytoplankton absorption and light penetration depth, which cannot be supplied by the current ocean colour satellite sensors. The spectral resolution of these sensors is not sufficient to extract the relevant information. The variation of phytoplankton absorption in ocean waters also affects the retrieval of chlorophyll a concentrations (a measure of phytoplankton biomass) derived from satellite data, which are important input data used in primary production models. Results by Bracher et al. (2006) show that specific phytoplankton absorption spectra as well as information on the light penetration depth can be derived by combining information from measurements of the two satellite instruments, MERIS with high spatial, and SCIAMACHY with high spectral resolution (both operating on board of the European environmental satellite ENVISAT).

Besides the analysis of satellite data and applied model studies, field measurements in the open ocean of phytoplankton pigment composition, optical characteristics of phytoplankton and other water constituents, reflectance and underwater light measurements are highly precise input parameters for the validation of results from the analyses of satellite data and modelling.

Thus the aim of this research project is to improve estimates of global marine primary production and the distribution of major phytoplankton functional groups by using remote sensing data in combination with *in-situ* measurements of ocean optics, phytoplankton productivity and composition and particulate organic carbon (POC). In particular, data will be collected during this cruise to improve our understanding of the oceans variability in optical properties and to improve/develop remote sensing algorithms for the investigated research area. Algorithms to retrieve POC from space are still very basic, but are of great importance for studies concerning biogeochemical cycles and the biological pump within the world's oceans because carbon and not chlorophyll are the bases for those studies. Through a better knowledge of the sinks and sources of CO<sub>2</sub> in the ocean a contribution will be made to a better

understanding of changes in the world's climate as well as to the understanding of the marine food web.

### **Work at sea**

#### **1. Water samples**

Water samples will be taken frequently (every 6 hours) from beneath the ship (moon pool) and at the stations from CTD/rosette casts and processed for various analyses:

- Water samples will be filtered onto GF/F filters for pigment analysis, particulate absorption measurements and POC.
- Water samples will be preserved for flow cytometry measurements later in the laboratory in Bremerhaven.
- Particulate absorption in suspension and absorption of Gelbstoff will be measured during the cruise using the point-source integrating-cavity absorption meter (PSICAM) (Röttgers et al. 2005).

#### **2. Online and *in-situ* optical measurements**

- A FastTracka Fast Repetition Rate Fluorimeter (FRRF) will be used in a flow-through system with water continuously pumped from the moon pool to provide online data of chlorophyll fluorescence during the cruise.
- A second FastTracka FRRF will be attached to the CTD to take measurements in the water column.
- Remote sensing reflectance will be measured firstly from onboard the ship with a set of three radiometers and secondly in the water column (0 - 150 m) at the stations.

### **Preliminary results**

#### **Distribution of phytoplankton**

The absorption and pigment samples are still waiting to be analysed, but generally the phytoplankton concentration was low during the cruise, especially in the open ocean and at the surface. The CTD profiles show that at most sites the fluorescence maximum laid beneath the surface (see Fig. 10.1 for examples).

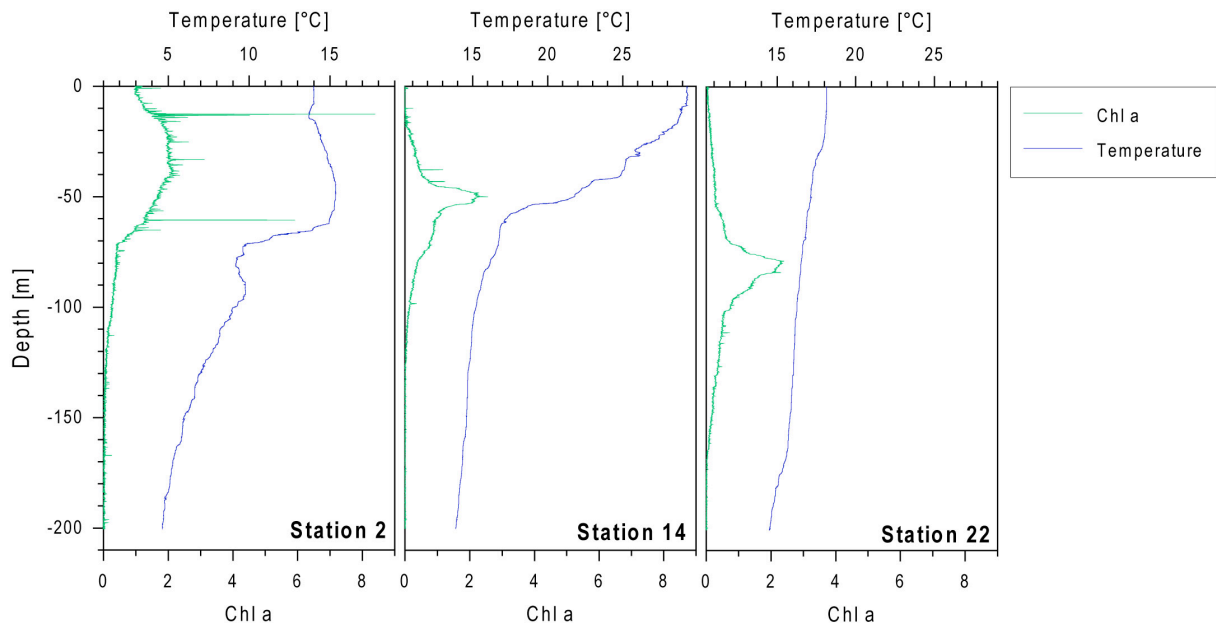


*Fig. 10.1: CTD profiles showing Chl a fluorescence (green) and temperature (blue) for three stations during the cruise. Approximate locations: Station 2: 42°S 54°W, Station 14: 3°N 24°W, Station 22: 36°N 12°W*

Unfortunately the FastTracka FRRF instruments were both damaged and could not be used on this cruise.

### Remote sensing reflectance

The *in-situ* data were collected with three hyperspectral RAMSES radiometers measuring:

- downwelling irradiance  $E_d$
- sky radiance  $L_s$  at a zenith angle of 40° and an azimuth angle of 135°
- upwelling radiance  $L_u$  at a nadir angle of 40° and the same azimuth angle as  $L_s$

MERIS data acquired within one day overpassing the *in-situ* sample location were considered and averaged (3 by 3 pixels). This led to several possible collocations per *in-situ* measurement. In Fig. 10.2 an example of compared *in-situ* and MERIS remote sensing reflectance is shown. Further validation and analysis of the data is in progress.

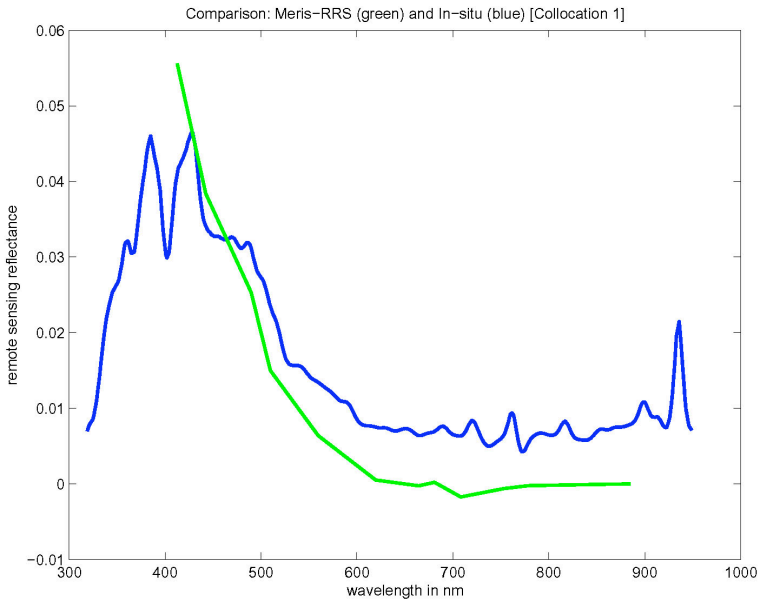


*Fig. 10.2: Example of collocated remote sensing reflectance data of in-situ (blue) and MERIS (green) from a “good” match-up station*

## References

- Bracher A., Vountas M., Dinter T., Röttgers R., Doerffer R., Burrows J.P. (2006) Retrieval of phytoplankton distribution and light absorption from space borne SCIAMACHY data using Differential Optical Absorption Spectroscopy. Proceedings of the Ocean Optics XVIII, 9-13 Oct 2006, Delta Centre Ville, Montreal, Canada
- Röttgers R., Schönfeld W., Kipp P.-R., Doerffer R. (2005) Practical test of a point-source integrating cavity absorption meter: the performance of different collector assemblies. Applied Optics, 44(26), 5549-5560.

## 10.2. MAX-DOAS measurements of atmospheric trace gases and water reflectance

### Objectives

In recent years global measurements of two chemical reactive hydrocarbons, formaldehyde (HCHO) and glyoxal (CHOCHO) with optical absorption spectroscopy from space became available (Wittrock et al. 2006). These measurements substantially add to our current knowledge on the global emissions of non-methane hydrocarbons (NMHC). NMHC are present at relatively low quantities in our atmosphere. Nevertheless, they play a key role in atmospheric photochemistry. For example, the oxidation of NMHC is significant for the formation of ozone in the troposphere (Heckel et al. 2005). In spite of their importance, their global source and sinks budgets particularly above the oceans are still not well understood.

Comparison of satellite measurements with model results have shown a very good agreement over the continents, but significant underestimation in the model over the

oceans. Here, the satellite measurements show clearly enhanced columns in some areas affected by continental outflow, indicating either a longer than modelled lifetime of HCHO and CHOCHO or more probably *in-situ* production by decomposition of long-lived organic compounds and marine sources of NMHC like phytoplankton.

In order to confirm (or falsify) the presence of these significant amounts of HCHO and CHOCHO over the oceans, dedicated MAX-DOAS measurements from ships like this during the latitudinal transect of ANT-XXIV/4 are very useful.

A close collaboration with the group from Heidelberg University is planned to provide trace gas data from different viewing directions.

### **Work at sea**

Multi-Axis Differential Optical Absorption Spectroscopy of tropospheric trace gases and water reflectance

- Vertical information of different trace gases (focus on CHOCHO and HCHO) can be derived from the inversion of the measurements for different elevation angles. Selected measurements towards the water surface will provide high resolution spectra, which should be helpful to improve the satellite trace gas and chlorophyll retrievals in the wavelength region from 330 to 500 nm.

### **References**

- Wittrock, F., Richter, A., Oetjen, H., Burrows, J.P., Kanakidou, M., Myriokefalitakis, S., Volkamer, R., Beirle, S., Platt, U., Wagner, T. (2006) Simultaneous global observations of glyoxal and formaldehyde from space, *Geophys. Res. Lett.*, **33**, L16804, doi:10.1029/2006GL026310
- Heckel, A., Richter, A., Tarsu, T., Wittrock, F., Hak, C. , Pundt, I., Junkermann, W., Burrows, J. P. (2005) MAX-DOAS measurements of formaldehyde in the Po-Valley, *Atmos. Chem. Phys.*, **5**, 909–918.

## 11. LONG-TERM CHANGES OF ABYSSAL TEMPERATURES IN THE VEMA CHANNEL

Walter Zenk (not on board)  
IFM-GEOMAR

### Objectives

Major quantities of Antarctic Bottom Water of the South Atlantic spread towards the equator as a deep western boundary current in the Argentine Basin. This process is supposed to play a paramount role in the global thermohaline circulation. On its flow from Antarctic sources to lower latitudes the densest water encounters the Rio Grande Ridge at about 31° S. This topographic constraint acts as a natural barrier for abyssal waters heading for the Brazil Basin farther to the north. The zonal alignment of the ridge is disrupted by a narrow gap called Vema Channel. Actually the Vema Channel features a conduit for advected bottom water (Fig. 11.1). Physical measurements at the Vema sill are therefore predestined for long-term observations of property and transport changes of Antarctic Bottom Water (Zenk et al., 1983). Records of over thirty years in the near-bottom layers in the Vema Channel depict a clear temperature increase beginning in the early 1990ies (Hogg and Zenk, 1997). This positive trend has been repeatedly documented in observations from local CTD stations gathered in international cooperation (Denker, 2007; Zenk and Morozov, 2007). An inventory list is given in Table 11.1.

During ANT-XXIV/4 it was the objective of the mini programme in physical oceanography to extend the collection of available hydro stations by an additional observation at the Vema Channel.

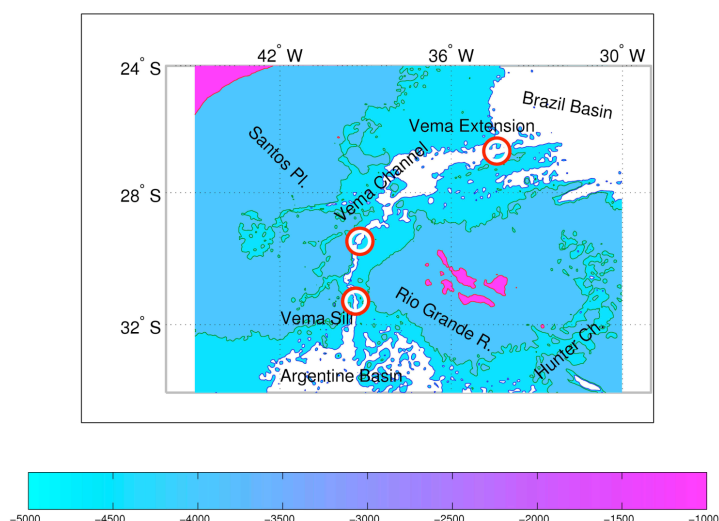


Fig. 11.1: Bottom topography of the Vema Channel. For better orientation the 4,600 m isobath is given by the transition between the coloured and the white areas. It demonstrates the conduit for Antarctic Bottom Water. The three circles show positions where repeated CTD stations were taken after 1991 (see Table 11.1). During ANT-XXIV/4 Polarstern revisited the Vema Sill (southern circle), i.e. the saddle point along the Vema Channel.

**Tab. 11.1:** Collection of hydro stations from Vema Channel 1925-2008. This list originally was published by Zenk and Morozov (2007). It was extended by two revisits since then. The locations of the three station categories on the right hand side are shown in Fig. 11.1.

Cruise/ Expedition	Country of ship or Institution	Date	No of Stations		
			Vema Sill	Santos Plateau	Vema Extension
Meteor, profile 2 Deutsche Atlantische Expedition	DE	Aug/1925	(1)		
Meteor, profile 4 Deutsche Atlantische Expedition	DE	Dec/1925	(1)		
Cato, leg 6 GEOSECS	US	Dec/1972	1		
Atlantis II-107,leg 2	US	Dec/1979	2		
Atlantis II-107,leg 8	US	Jun/1980	4		
Washington Marathon / 9	US	Dec/1984	4		
Meteor 15, leg 1	DE	Jan/1991	6		
Meteor 22, leg 4	DE	Dec/1992	5		1
Polarstern ANT 12/1	DE	Nov/1994	1		
Meteor 34, leg 3	DE	Mar/1996	3	1 b	1
Meteor 41, leg 3	DE	Apr/1998	4		1
Meteor 46	DE	Feb/2000	2 c		
Ak. Ioffe 11, leg 1	RU	Nov/2002	7	2	
Ak. S. Vavilov 17, leg 1	RU	Nov/2003	6	2	5
RSS Discovery 276	UK/DE	Dec/2003	1	1	1
Ak. Ioffe 16, leg 1	RU	Nov/2004	5		1
Ak. Ioffe 17, leg 1	RU	Mar/2005	5		
Polarstern ANT 22/5	DE	May/2005	5	1	1
Ak. Ioffe 19, leg 1	RU	Nov/2005	5		
Ak. Ioffe 22, leg 1	RU	Oct/2006	1		
James Clark Ross 160	UK/DE	May/2007	1		
<b>Polarstern ANT XXIV/4</b>	<b>DE</b>	<b>Apr/2008</b>	<b>1</b>		
Sums			71	7	11

## Work at sea

The aim to continue the hydrographic long-term abyssal series from the entrance of the Vema Channel was achieved on 26 April 2008. With the thankful help of B. Schmitt *Polarstern* occupied the choke point station on the eastern side the Vema Sill where the CTD probe was lowered down to the sea bed (see List of Stations in Annex A.4 of this Report).

## Preliminary results

Figure 11.2 depicts the series of lowest potential temperatures collected from critical locations at the mouth of the Vema Channel since 1972. Since 1991 all shown data points were collected exactly at the same area of the Vema Sill, i.e. the location where the coldest core of Antarctic Bottom Water hugs against the eastern wall of the channel (southern circle in Fig. 11.1). The last data point on the right labelled by a circle originates from ANT-XXIV/4.

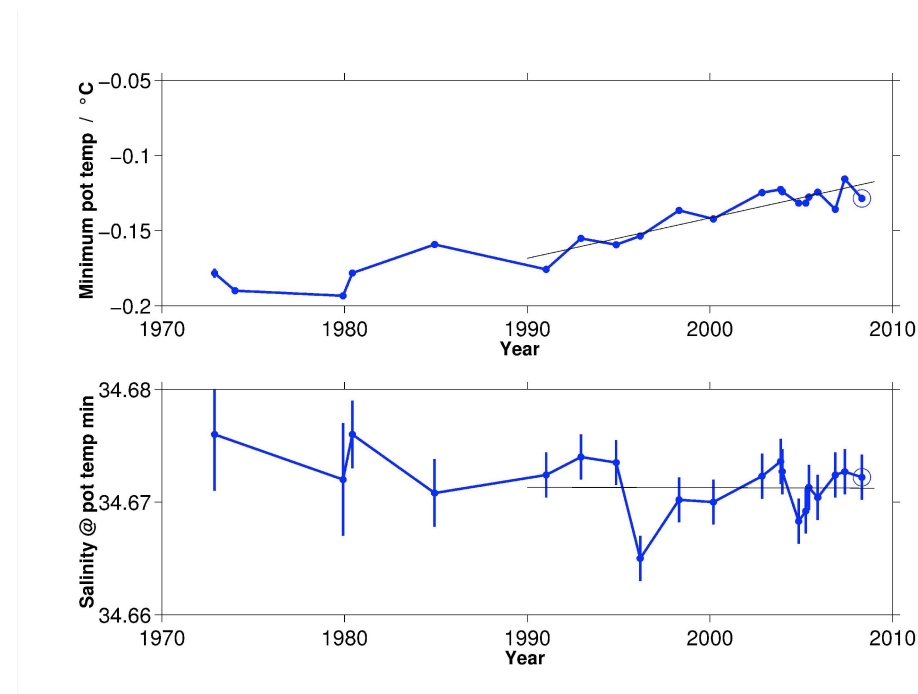


Fig. 11.2: Potential temperature (top) and salinity (bottom) changes of the coldest Antarctic Bottom Water, i.e. Weddell Sea Deep Water at the eastern side of the Vema Channel. This figure is an update of the corresponding graph in Zenk and Morozov (2007). The slope in temperature since 1991 amounts to +2.7 milliKelvin/y.

Below the temperature series we show corresponding salinity series with error estimates. This curve is noisy. It allows no reliable conclusion on long-term changes of the abyssal water density. For details see Zenk and Morozov (2007).

In Fig. 11.3 we present the collection of potential temperature profiles below 3,400 dbar from the Vema Sill. Where more than one profile is shown hydrographic sections across the channel were taken. Results are given as overplots. The vertical

lines at 0.2° and 2.0° C in every subplot show the expected range of Weddell Sea Deep Water and the upper limit of Antarctic Bottom Water, respectively.

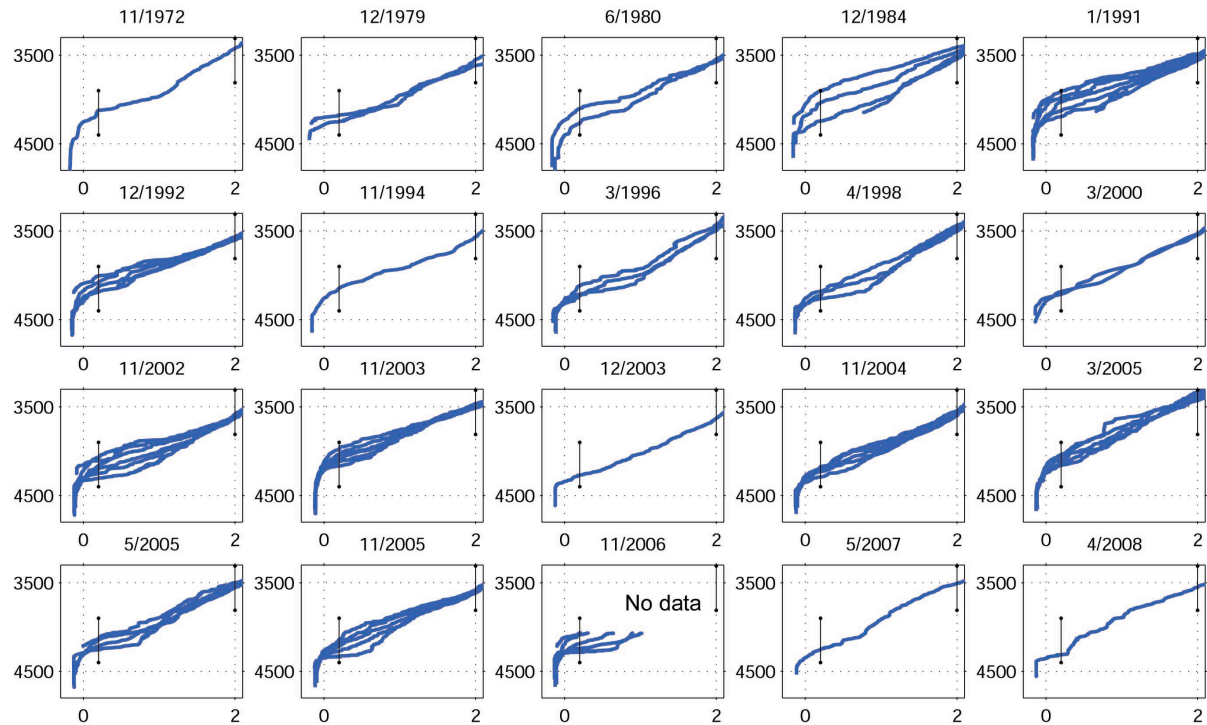


Fig. 11.3: Collection of potential temperature profiles from the Vema Channel, 1972-2008. x-axis in °C, y-axis for pressure in dbar

## References

- Zenk, W., Speer, K.G., Hogg, N.G. (1993) Bathymetry at the Vema Sill, *Deep-Sea Res., I*, **40**, 1925-1933.
- Hogg, N. G., Zenk, W. (1997), Long-period changes in the bottom water flowing through Vema Channel, *J. Geophys. Res.*, **102**(C7), 15639-15646.
- Denker, C. (2007) Schwankungen von Wassermasseneigenschaften an der Schwelle des Vema-Kanals. Dipl. Arbeit, CAU Kiel, 62 S.
- Zenk, W., Morozov, E. (2007) Decadal warming of the coldest Antarctic Bottom Water flowing through the Vema Channel, *Geophys. Res. Letters*, **34**, L14607, doi:10.1029/2007/GLR030340.

---

## **APPENDIX**

### **A.1 PARTICIPATING INSTITUTIONS**

### **A.2 CRUISE PARTICIPANTS**

### **A.3 SHIP'S CREW**

### **A.4 STATION LIST**

---

## A.1 BETEILIGTE INSTITUTE/ PARTICIPATING INSTITUTIONS

	<b>Adresse Address</b>
AWI	Alfred-Wegener-Institut für Polar- und Meeresforschung Am Handelshafen 12 27570 Bremerhaven/ Germany
DWD	Deutscher Wetterdienst Geschäftsbereich Wettervorhersage Seeschifffahrtsberatung Bernhard Nocht Str. 76 20359 Hamburg Germany
DZMB	Deutsches Zentrum für marine Biodiversität Biozentrum Grindel und Zoologisches Museum Martin-Luther-King-Platz 3 20146 Hamburg/ Germany
GKSS	GKSS Forschungszentrum Geesthacht, Institut Max Planck- Str. 1, 21502 Geesthacht/ Germany
IFM-GEOMAR	Leibniz-Institut für Meereswissenschaften IFM-GEOMAR Düsternbrooker Weg 20 24105 Kiel/ Germany
IGMK	Institut für Geophysik und Meteorologie der Universität Köln, Kerpener Str. 13 50937 Köln / Germany
IUP-HB	Institut für Umweltphysik Universität Bremen Otto-Hahn-Allee, NW1 D-28334 Bremen/ Germany

---

**Adresse****Address**

---

LGGE	Laboratoire de Glaciologie et Géophysique de l'Environnement (UMR 5183) 54, rue Molière 38402 - Saint Martin d'Hères cedex / France
MPI-Met	Max-Planck-Institut für Meteorologie Bundesstraße 53 20146 Hamburg Germany

---

## A.2 FAHRTTEILNEHMER / CRUISE PARTICIPANTS

Name/ Last name	Vorname/ First name	Institut/ Institute	Beruf/ Profession
Bentama	Laila	GKSS	Student, biology
Bumke	Karl	IFM-GEOMAR	Meteorologist
El Naggar	Saad	AWI	Physicist
Erbländ	Joseph	LGGE	Chemist
Gehrung	Martina	GKSS	Engineer
Grefe	Imke	IFM-GEOMAR	Student, biology
Hieronymi	Martin	IFM-GEOMAR	Meteorologist
Kalisch	John	IFM-GEOMAR	Meteorologist
Kinne	Stefan	MPI-Met	Meteorologist
Lengfeld	Katharina	IFM-GEOMAR	Student, meteorology
Macke	Andreas	IFM-GEOMAR	Physicist
Müller	Eugen	DWD	Meteorologist
Niessen	Frank	AWI	Geologist
Pospichal	Bernhard	IGMK	Meteorologist
Schmitt	Bettina	AWI	Biologist
Schulte in den Bäumen	Hagen	IUP	Physicist
Sonnabend	Hartmut	DWD	Technician
Steinhoff	Tobias	IFM-GEOMAR	Chemist
Taylor	Marc	IUP	Student, biology
Theis	Anja	IUP	Student, physics
Véliz Moraleda	Fredy	AWI	Student, biology
Wittmann	Astrid	AWI	Biologist
Zoll	Yann	IFM-GEOMAR	Meteorologist

## A.3 SCHIFFSBESATZUNG / SHIP'S CREW

No.	Name	Rank
01.	Schwarze, Stefan	Master
02.	Spielke, Steffen	1.Offc.
03.	Farysch, Bernd	Ch. Eng.
04.	Peine, Lutz G.	2.Offc./L.
05.	Dugge Heike	3.Offc.
06.	Sokoll, Herbert	Doctor
07.	Hecht, Andreas	R.Offc.
08.	Minzlaff, Hans-Ulrich	1.Eng.
09.	Sümnight, Stefan	2.Eng.
10.	Schaefer, Marc	3.Eng.
11.	Scholz, Manfred	Elec Eng.
12.	Himmel, Frank	Elec Eng.
13.	Muhle, Helmut	Electron.
14.	Nasis, Ilias	Electron.
15.	Loidl, Reiner	Boatsw
16.	Reise, Lutz	Carpenter
17.	Bäcker, Andreas	A.B.
18.	Guse, Hartmut	A.B.
19.	Hagemann, Manfred	A.B.
20.	Schmidt, Uwe	A.B.
21.	Stutz, Heinz-Werner	A.B.
22.	Vehlow, Ringo	A.B.
23.	Wende, Uwe	A.B.
24.	Winkler, Michael	A.B.
25.	Preußner, Jörg	Storek.
26.	Elsner, Klaus	Mot-man
27.	Hartmann, Ernst-Uwe	Mot-man
28.	Ipsen, Michael	Mot-man
29.	Pinske, Lutz	Mot-man
30.	Voy, Bernd	Mot-man
31.	Müller-Homburg, R.-D.	Cook
32.	Martens, Michael	Cooksman
33.	Silinski, Frank	Cooksman
34.	Jürgens, Monika	1.Stwdess
35.	Wöckener, Martina	Stwdss/Kr
36.	Czyborra, Bärbel	2.Stwdess
37.	Gaude, Hans-Jürgen	2.Steward
38.	Huang, Wu-Mei	2.Steward
39.	Möller, Wolfgang	2.Stwdard
40.	Silinski, Carmen	2.Stwdess.
41.	Yu, Kwok Yuen	Laundrym.
42.	Paulisch, Catharina	Trainee/E

## A.4 STATIONSLISTE / STATION LIST PS 71

Station PS71/	Date	Time	Pos. Lat	Pos. Lon	Depth [m]	Gear Abbreviation	Action	Comment
-259	21.04.08	17:00	-45,70	-58,5	2593	CTD/Radiometer	CTD and Radiometer to 200 m, back on deck	
-260	22.04.08	17:00	-42,77	-54,3	5432	CTD/Radiometer	CTD and Radiometer to 200 m, back on deck	
261	23.04.08	17:00	-39,64	-50,02	5381	CTD/Radiometer	CTD and Radiometer to 200 m, back on deck	
-262	24.04.08	16:00	-36,75	-46,25	5034	CTD/Radiometer	CTD and Radiometer to 200 m, back on deck	
-263	25.04.08	16:00	-33,55	-42,18	4929	CTD/Radiometer	CTD and Radiometer to 200 m, back on deck	
-264	26.04.08	10:00	-31,22	-39,34	4990	CTD	CTD to bottom, back on deck	CTD grounded
-265	27.04.08	16:00	-26,7	-36,72	4505	CTD/Radiometer/ Underwater Camera	CTD and Radiometer to 200 m, back on deck, UW-Cam up to 25 m	
-266	28.04.08	15:00	-23,04	-34,67	4242	CTD/Radiometer	CTD and Radiometer to 200 m, back on deck	
-267	29.04.08	15:00	-19,18	-32,75	4145	CTD/Radiometer/ Underwater Camera	CTD and Radiometer to 200 m, back on deck, UW-Cam up to 15 m	
-268	30.04.08	15:00	-15,24	-31,15	4721	CTD/Radiometer/ Underwater Camera	CTD and Radiometer to 200 m, back on deck, UW-Cam up to 15 m	
-269	01.05.08	15:00	-11,26	-29,56	5422	CTD/Radiometer/ Underwater Camera	CTD and Radiometer to 200 m, back on deck, UW-Cam up to 30 m	
-270	02.05.08	15:00	-7,26	-27,99	5580	CTD/Radiometer/ Underwater Camera	CTD and Radiometer to 200 m, back on deck, UW-Cam up to 25 m	
-271	03.05.08	14:00	-3,7	-26,6	5380	CTD/Radiometer/ Underwater Camera	CTD and Radiometer to 200 m, back on deck, UW-Cam up to 25 m	
-272	05.05.08	14:00	3,93	-24,33	4292	CTD/Radiometer/ Underwater Camera	CTD and Radiometer to 200 m, back on deck, UW-Cam up to 25 m	
-273	06.05.08	14:00	7,85	-23,49	4646	CTD/Radiometer/ Underwater Camera	CTD and Radiometer to 200 m, back on deck, UW-Cam up to 25 m	
-274	07.05.08	14:00	11,99	-22,6	4981	CTD/Radiometer	CTD and Radiometer to 200 m, back on deck	
-275	08.05.08	13:00	15,88	-21,74	3856	CTD/Radiometer	CTD and Radiometer to 200 m, back on deck	
-276	09.05.08	13:15	19,98	-20,83	3702	CTD/Radiometer/ Underwater Camera	CTD and Radiometer to 200 m, back on deck, UW-Cam up to 25 m	
-277	10.05.08	13:00	23,84	-20,05	3763	CTD/Radiometer/ Underwater Camera	CTD and Radiometer to 200 m, back on deck, UW-Cam up to 25 m	

**APPENDIX**

---

<b>Station PS71/</b>	<b>Date</b>	<b>Time</b>	<b>Pos. Lat</b>	<b>Pos. Lon</b>	<b>Depth [m]</b>	<b>Gear Abbreviation</b>	<b>Action</b>	<b>Comment</b>
-278	11.05.08	12:00	26,34	-17,22	3595	CTD/Radiometer/ Underwater Camera	CTD and Radiometer to 200 m, back on deck, UW- Cam up to 25 m	
-279	13.05.08	12:00	32,76	-14,08	4257	CTD/Radiometer/ Underwater Camera	CTD and Radiometer to 200 m, back on deck, UW- Cam up to 25 m	
-280	14.05.08	12:00	36,56	-12,76	2703	CTD/Radiometer/ Underwater Camera	CTD and Radiometer to 200 m, back on deck, UW- Cam up to 25 m	
-281	15.05.08	12:00	40,81	-10,68	4472	CTD/Radiometer/ Underwater Camera	CTD and Radiometer to 200 m, back on deck, UW- Cam up to 25 m	
-282	16.05.08	12:00	44,99	-8,45	4850	CTD/Radiometer/ Underwater Camera	CTD and Radiometer to 100m, back on deck, CTD 2 to 50 m-> water for crab tanks, UW-Cam up to 15 m	

Die "Berichte zur Polar- und Meeresforschung" (ISSN 1866-3192) werden beginnend mit dem Heft Nr. 569 (2008) ausschließlich elektronisch als Open-Access-Publikation herausgegeben. Ein Verzeichnis aller Hefte einschließlich der Druckausgaben (Heft 377-568) sowie der früheren "Berichte zur Polarforschung" (Heft 1-376, von 1982 bis 2000) befindet sich im Internet in der Ablage des electronic Information Center des AWI (**ePIC**) unter der URL <http://epic.awi.de>. Durch Auswahl "Reports on Polar- and Marine Research" auf der rechten Seite des Fensters wird eine Liste der Publikationen in alphabetischer Reihenfolge (nach Autoren) innerhalb der absteigenden chronologischen Reihenfolge der Jahrgänge erzeugt.

*To generate a list of all Reports past issues, use the following URL: <http://epic.awi.de> and select the right frame to browse "Reports on Polar and Marine Research". A chronological list in declining order, author names alphabetical, will be produced, and pdf-icons shown for open access download.*

#### **Verzeichnis der zuletzt erschienenen Hefte:**

**Heft-Nr. 578/2008** — "Benthic organic carbon fluxes in the Southern Ocean: regional differences and links to surface primary production and carbon export", by Oliver Sachs

**Heft-Nr. 579/2008** — "The Expedition ARKTIS-XXII/2 of the Research Vessel 'Polarstern' in 2007", edited by Ursula Schauer.

**Heft-Nr. 580/2008** — "The Expedition ANTARKTIS-XXIII/6 of the Research Vessel 'Polarstern' in 2006", edited by Ulrich Bathmann

**Heft-Nr. 581/2008** — "The Expedition of the Research Vessel 'Polarstern' to the Antarctic in 2003 (ANT-XX/3)", edited by Otto Schrems

**Heft-Nr. 582/2008** — "Automated passive acoustic detection, localization and identification of leopard seals: from hydro-acoustic technology to leopard seal ecology", by Holger Klinck

**Heft-Nr. 583/2008** — "The Expedition of the Research Vessel 'Polarstern' to the Antarctic in 2007 (ANT-XXIII/9)", edited by Hans-Wolfgang Hubberten

**Heft-Nr. 584/2008** — "Russian-German Cooperation SYSTEM LAPTEV SEA: The Expedition Lena - New Siberian Islands 2007 during the International Polar Year 2007/2008", edited by Julia Boike, Dmitry Yu. Bolshiyanov, Lutz Schirmeister and Sebastian Wetterich

**Heft-Nr. 585/2009** — "Population dynamics of the surf clams *Donax hanleyanus* and *Mesodesma mactroides* from open-Atlantic beaches off Argentina", by Marko Herrmann

**Heft-Nr. 586/2009** — "The Expedition of the Research Vessel 'Polarstern' to the Antarctic in 2006 (ANT-XXIII/7)", edited by Peter Lemke

**Heft-Nr. 587/2009** — "The Expedition of the Research Vessel 'Maria S. Merian' to the Davis Strait and Baffin Bay in 2008 (MSM09/3), edited by Karsten Gohl, Bernd Schreckenberger, and Thomas Funck

**Heft-Nr. 588/2009** — "Selected Contributions on Results of Climate Research in East Germany (the former GDR)", edited by Peter Hupfer and Klaus Dethloff

**Heft-Nr. 589/2009** — "The Expedition of the Research Vessel 'Polarstern' to the Arctic in 2008 (ARK-XXIII/1)", edited by Gereon Budéus

**Heft-Nr. 590/2009** — "The Expedition of the Research Vessel 'Polarstern' to the Arctic in 2008 (ARK-XXIII/2)", edited by Gerhard Kattner

**Heft-Nr. 591/2009** — "The Expedition of the Research Vessel 'Polarstern' to the Antarctic in 2008 (ANT-XXIV/4)", edited by Andreas Macke